Journal of Materials Chemistry B

Accepted Manuscript

ROYAL SOCIETY OF CHEMISTRY

www.rsc.org/materialsB

Journal of
Materials Chemistry B

RSCPublishing

ARTICLE

Engineering of biomimetic nanofibrous matrices for drug delivery and tissue engineering

Cite this: DOI: 10.1039/x0xx00000x

Chuanglong He,* Wei Nie and Wei Feng

Received 00th January 2014,
Accepted 00th January 2014

DOI: 10.1039/x0xx00000x

www.rsc.org/

Biomimetic nanofibers have emerged as promising candidates for drug delivery and tissue engineering applications. In this paper, recent advances on the fabrication and application of biomimetic nanofibers as drug carriers and scaffolding materials are reviewed. First, we delineate the three popular nanofiber fabrication techniques including electrospinning, phase separation and molecular self-assembly, covering the principal materials used for different techniques and surface functionalization strategies for nanofibers. Furthermore, we focus our interest on the nanofiber-based delivery strategies and underlying kinetics for growth factors and other bioactive molecules, following which we summarize the recent advances in the development of these nanofibrous matrices for bone, vascular and neural tissue engineering applications. Finally, research challenges and future trends in the related areas are discussed.

1. Introduction

Tissue engineering combines the principles and technologies from the life, material and engineering sciences to develop functional substitutes for damaged tissues and organs. Its underlying concept is to combine a scaffold with living cells and/or bioactive molecules to form a living construct promoting the repair and regeneration of human tissue. To be successful in tissue regeneration, the living cells should be effectively reorganized into a three-dimensional (3D) scaffold with morphological and physiological features resembling those *in vivo*.[1] In this context, the scaffold should be properly designed to provide more than only temporary physical support for cells but also the correct mechanical, topographical and biological cues to regulate cellular responses and direct tissue growth.[2] With an ever expanding knowledge of cell-matrix interactions in natural tissues, the last few years has evidenced a paradigm shift in design criteria of ideal tissue engineered scaffolds, a variety of biomimetic scaffolds capable of recapitulating critical structural and biological features of natural extracellular matrix (ECM) are currently being developed.[3,4]

Cells are supported *in vivo* by a 3D network of ECM, which contains various proteins, growth factors and polysaccharides that contributes physical structure and a biochemical context to the extracellular microenvironment (Fig. 1).[5] The major ECM components such as collagen and elastin exist in the form of interwoven nanofibers with diameters ranging from tens to hundreds of nanometers, which are covered with nanoscale adhesion proteins such as laminin and fibronectin that provide specific binding sites for cell adhesion.[1,3,5,6] Such a nanoscale structure of the ECM provides a fibrillar matrix network to support cells and present an instructive background to guide their behavior. Cells can interact with their ECM microenvironments by receptor-mediated interactions, the sequestration of growth factors by the ECM, spatial cues and mechanical fore transduction, to trigger various intracellular signaling pathways that regulate various essential cell behaviors and cell fate determination.[3,7,8] Therefore, it is highly desirable to develop an engineered ECM analog that incorporates nanoscale structural, biochemical and biomechanical cues required for optimal tissue regeneration. Recent advances in the fabrication of nanofibers make it possible to engineer novel scaffolding materials with these levels of complexities.

Polymer nanofibers have been fabricated using several different techniques including physical, chemical, thermal and electrostatic fabrication techniques.[9] The dominating techniques capable of producing ECM-mimicking nanofibrous scaffold are electrospinning,[10] thermally induced phase separation (TIPS)[11] and molecular self-assembly.[12] Due to their unique properties such as large specific surface-to-volume ratio and the capacity of mimicking native ECM, biomimetic nanofibers are highly suitable as scaffolds for tissue regeneration and carriers for drug delivery.[6,13] Consequently, it comes to a common view that tissue scaffolds and drug carriers developed by these nanofibers had great potential in biomedical application.

The aim of this review is to provide an overview of the recent progress in the design, fabrication and modification of biomimetic nanofibers for drug delivery and tissue engineering applications, with a particular focus on fabricating electrospun nanofibers in a biomimetic perspective. First, we present a comprehensive description to the three main nanofiber fabrication techniques including electrospinning, TIPS and molecular self-assembly, covering the principal materials used for different fabrication techniques and surface functionalization strategies for nanofibers, with emphasis on issues for biomimetic design. Next, we highlight the nanofiber-based delivery strategies and underlying kinetics for growth factors and other bioactive molecules, following which we summarize the recent advances in the development of these nanofibrous matrices for bone, vascular and neural tissue engineering applications. Finally, we conclude with current

challenges and future directions in the development of biomimetic nanofibers for drug delivery and tissue engineering applications.

2. Biomimetic nanofibers

2.1 Preparation methods

Depending on different materials used, three well-established techniques can be applied for fabrication of biomimetic nanofibers. Although all of these techniques enable to produce 3D nanofibrous scaffolds suitable for use in tissue engineering applications, each has inherent advantages and limitations.[14] With respect to their individual advantageous, TIPS generally requires minimal equipment,[15] molecular self-assembly can produce nanofibers with a smaller size,[16] but electrospinning is the most widely adopted technique for nanofiber fabrication because of its versatility and flexibility and is the focus of this review.

2.1.1 Electrospinning. Electrospinning, which utilizes electrostatic forces to create nanofibers, have been invented over 100 years.[17] A typical electrospinning apparatus includes a high voltage power source, a syringe pump, a metallic spinneret and a conductive collector (Fig. 2a).[18] In order for electrospinning to occur, a high voltage is applied to create an electric field between polymer solution and the grounded collector. With the use of a syringe pump, the polymer solution is delivered to the tip of spinneret at a constant rate. The polymer droplet is initially held by its surface tension at the tip and gradually drawn from the tip as the electric field increased. When the electrostatic force is sufficient to overcome the surface tension, a taylor cone forms and a fine jet ejects from its surface toward the collector (Fig. 2a). The polymer jets travel from the tip to the collector allowing the solvent to evaporate, thus the solid nanofibers formed and deposited on the collector (Fig. 2d). The morphology and diameter of the resulting nanofibers can be tuned by the variation of the processing parameters, which includes the intrinsic properties of polymer solution such as the nature and molecule weight of the polymer, the rheological properties of polymer solution (concentration, surface tension, elasticity and electrical conductivity), various operational conditions such as applied voltage, feeding rate for the polymer solution and collecting distance between spinneret tip to collector, as well as ambient parameters such as temperature, humidity and air velocity.[10,19] The diameter of the electrospun nanofibers is mainly dependent on the concentration and viscosity of polymer solution, applied voltage and collecting distance. Concurrently, the porosity and pore sizes of the resulting nanofibous scaffolds can be regulated by fiber diameter and their packing density. As a result, the feeding rate for the polymer solution exerts an impact on the fiber porosity and geometry, and some bead-like defects are frequently observed at high feeding rate due to the insufficient solvent evaporation. In addition, the collecting distance between spinneret tip to collector is considered as another factor contributing to the diameter and morphology of nanofibers. The fiber diameter tends to decrease with increasing tip-collector distance, while some bead-like or conglutinated fibers may be occurred at high collecting distance.[10,20]

The spinneret system can be suitably modified to produce diverse nanofibers such as blend and core-sheath nanofibers, which can be realized by using a multiple spinneret system[21-23] (Fig. 2b) and a coaxial one (Fig. 2c).[24,25] Compared with typical electrospinning setup, multiple spinneret system allows the same polymer solution to simultaneously eject from different spinnerets, or the different polymer solutions to separately eject from different spinnerets (Fig. 2b), hence it more suitable for larger-scale production or fabrication of multi-component fibers (Fig. 2e). While coaxial spinneret system, which consisted of a syringe-like apparatus with an inner capillary coaxially placed inside an outer one (Fig. 2c), is a feasible and versatile method to prepare core-sheath nanofibers (Fig. 2f).[26,27] Apart from multiple and coaxial electrospinning, some needless electrospinning setups were recently invented for the mass nanofiber production, including bubble electrospinning[28] and rotating spinnerets combined electrospinning.[29,30]

Recently, many modified electrospinning techniques have been developed to meet certain requirements. By improving the spinneret design and collecting apparatus, nanofibers with different shapes and structural characteristics were obtained for specific tissue regeneration and drug delivery applications. Rotating collectors were frequently employed for collection of the aligned nanofibers,[13,31,32] which are mainly composed of a metal cylinder collector that can rotate by motor driving (Fig. 3a). When the fiber jets deposited on the rotating collector, the generated centrifugal force can induce the orderly deposition of nanofibers. The other variations based on this method were also developed, including a rotating wheel[13,32,33] (Fig. 3b) or a rotating wire drum (Fig. 3c).[34] During electrospinning, a strongly concentrated electrostatic field can be created by using a rotating wheel collector, which directs the charged jet toward the knife-edge of the wheel, resulting in a well-aligned fibrous mat along the edges of the disc.[13] The as-prepared aligned nanofibers can be used for the tissue suturing[13,32] and tissue regeneration[35] applications. To fabricate nanofibrous scaffolds with complex geometries, a broad array of collecting apparatus were also proposed, such as counter electrodes array and parallel ring collector for fiber assembles (Fig. 3d and e),[36,37] as well as liquid or dynamic liquid deposition for nanoyarn fabrication.[38-40] In addition, the patterned electrospun nanofibers and 3D nanofibrous architecture can be fabricated using a continuous conductive collector with patterned protrusions (Fig. 3f and g).[41-43]

2.1.2 Phase separation. TIPS is a prevailing method to generate nanofibers in the same size range as natural ECM collagen (50-500 nm), in which inter-connected macroporous architecture can be facilely made by combined with other techniques such as porogen leaching[44-46] and solid freeform fabrication,[47] allowing sufficient space for cell migration, matrix deposition and tissue formation.[48-52] The principle of this technique is that a homogeneous polymer-solvent system would be thermodynamically unstable under some specific conditions, such as exposure of the solution to another immiscible solvent or rapid cooling the solution below a bimodal solubility curve. As a result, polymer solution is separated into a polymer-rich phase and a polymer-lean

phase. After removal of solvent, the polymer-rich phase solidifies and forms a porous scaffold. Furthermore, the unique nanofibrous structure can be produced by suitably manipulating the phase separation process such as the gelation and solvent exchanging process (Fig. 4). The technique was initially validated with aliphatic polyesters such as poly(L-lactide) (PLLA),[52] but several other polymers including copolymers of PLLA and poly(ε-caprolactone) (PCL), such as poly(ε-caprolactone)-block-poly(L-lactide) (PCL-b-PLLA)[53] and poly(ε-caprolactone)-block-poly(L-lactic acid-co-ε-caprolactone) (PCLA),[54] polyhydroxyalkanoate,[55] chitosan[56] and gelatin[45,57] have been successfully processed into nanofibers by TIPS technique. Despite the advantages, this approach has limitations in its ability to develop a wide spectrum of polymer nanofibers for broader biomedical applications.

2.1.3 Molecular self-assembly. Unlike electrospinning and TIPS, molecular self-assembly is a bottom-up approach to create nanofibers from small molecules, proteins, peptides and nucleic acids. The process, resembling those that occur naturally in biological systems, generally involves the spontaneous organization of individual components into ordered and stable aggregating structures.[58] Self-assembling process is mediated by non-covalent forces including van der Waals forces, hydrogen bonds and electrostatic forces.[12] So far several different types of peptide-based self-assembly fibrous biomaterials have been demonstrated, which mainly include amyloid-like structures, α-helical assemblies and peptide amphiphiles (PAs).[59] Among these, PAs containing both a hydrophobic tail group and a hydrophilic head group are a common building block for self-assembled nanofibers. Stupp and co-works fist demonstrated that this type of molecules could be self-assembled into cylindrical micelles or peptide nanofibers.[16] For efficient self-assembly, PAs were designed to include five key structure features: a 16-carbon alkyl tail providing the hydrophobic driving force to trigger self-assembly, a peptide region with four consecutive cysteine residues to form disulfide bonds for polymerization, a head group region with three glycine residues to provide flexibility, a phosphorylated serine residue that helps to direct mineralization, and an Arg-Gly-Asp (RGD) sequence to facilitate cell adhesion. The self-assembly of these PA monomers into cylindrical nanofibers can be triggered by a change in pH or the concentration of divalent ions, which neutralize the electrostatic repulsion between molecules and to allow for clustering of the hydrophobic tails in the core, while exposing the hydrophilic heads on the exterior of the fiber (Fig. 5a-d). These PAs can be further modified by changing the alkyl tail length and peptide amino acid composition, and create nanofibers with varying morphology, surface and bioactivity.[60] The resulting PA nanofibers possess fiber dimensions similar to that of native ECM and can form gel networks at low media concentrations, allowing for 3D cell encapsulation.[61] The self-assembly approach can be tailored *in vivo* to create an injectable scaffold for *in situ* scaffold formation.[62,63] Furthermore, several bioactive cues can be presented simultaneously by co-assembling multiple PA molecules bearing different signals.[64] Recent works have increasingly demonstrated potential biomedical applications for a variety of PA nanofibers. For example, different PA fibers have been used as tunable scaffolds for the tissue engineering of bone,[65,66] cartilage,[67] blood vessel[68] and nerve,[69-72] and as the platforms or carriers for the controlled release of growth factors and therapeutic agents.[73,74]

Ionic self-complementary peptides can also serve as building blocks to construct nanofibers.[75-78] These peptides have alternating positively and negatively charged amino acids, such as 16-amino acid peptides RADA16-I (Ac-RADARADARADARADA-NH_2) and RADA16-II (Ac-RARADADARARADADA-NH_2), which form β-sheet structures in aqueous solution with two distinct hydrophilic and hydrophobic surfaces. When expose these peptides to a salt solution or to physiological media, they can be self-assembled into hydrogels with interwoven nanofibrous structure (Fig. 5d).[12] Such a scaffold is not only highly porous having a pore size of 5-200 nm but also possesses an extremely high water content of more than 99.5%, and thus is particularly suitable for the cell growth and the delivery of bioactive molecules in various fields of tissue engineering.[75,77,79-82] In addition, the engineering of collagen-like[83-85] and elastin-like[86-88] polypeptides as building blocks for self-assembled nanofibers with specific structural and mechanical properties is of great interest to the biomedical community. Despite these impressive advances, however, the self-assembly process is still a time-consuming and relatively expensive approach for nanofiber fabrication at the moment.

2.2 Nanofibers from different polymers

Polymer nanofibers represent excellent structures for the design of tissue engineering scaffolds and drug delivery carriers because of their unique characteristics such as very large surface area-to-volume ratio, high porosity with very small pore size, and tunable structural and mechanical properties. Most importantly, their nanoscale fibrous structure closely resembles the native ECM niche that cells grow in and provides appropriate physical cues for manipulating cellular functions. A large variety of biocompatible polymers can be formed into nanofibrous structures by using several different processing techniques. Among which, phase-separated nanofibers are currently restricted to a narrow range of polymers, whereas self-assembled nanofibers are mainly originated from peptides, PAs, peptide-polymer conjugates and proteins. In contrast, electrospinning is the most versatile technique for nanofiber production that nanofibers can be produced from a wide range of materials including natural and synthetic polymers, ceramics and their composites. To date, more than 200 polymers have been successfully electropun into nanofibers for various potential applications.[89] For building up more biomimetic platforms, numerous bioactive molecules and therapeutic drugs can be introduced into polymer nanofibers by either *in situ* incorporation or by post-modification processes.

The most widely used synthetic polymers available for electrospinning are linear aliphatic polyesters, such as PLLA, poly (glycolic acid) (PGA), PCL and their copolymers. These synthetic polymers nanofibers allow for easy tailoring of their mechanical, architectural and degradation properties, but they are generally hydrophobic and lack active binding sites for cell adhesion and therefore require additional modifications. In addition, several water-soluble synthetic polymers such as poly(N-

vinylpyrrolidone) (PVP),[90] poly(ethylene glycol) (PEG),[91] polyvinyl alcohol (PVA)[92,93] and polyethylene oxide (PEO)[94] are also the ideal candidates to fabricate nanofibers for biomedical applications, especially for use as drug carriers. For example, Dai et al.[95] applied blend electrospinning to prepare emodin-incorporated PVP nanofibers. *In vivo* test and histological evaluation revealed that the emodin-loaded nanofibrous membrane had an accelerated therapeutic effect. Li et al.[92] developed a rapid-dissolving drug delivery system by using electrospun PVA as the fiber-forming polymer and drug carrier. The model drugs including caffeine and riboflavin were evenly distributed into the medicated nanofibers, and the *in vitro* dissolution test showed that the encapsulated drugs can be released in a burst manner from the PVA nanofibrous carriers. In addition, PEO was usually severed as an additive or a booster to improve the spinnability of some refractory polymers that are not amenable to electrospinning.[96-100]

Nanofibers from natural polymers, such as collagen,[101-103] gelatin,[104,105] elastin,[106] silk fibroin,[107-111] spider silk,[112] fibrinogen,[113-115] chitosan,[116-118] hyaluronic acid[119] and alginate,[120] represent more attractive alternative for biomimetic applications. Many of these materials contain specific cell-binding sites that are very beneficial for cell attachment, proliferation and even differentiation. However, natural polymers also have some limitations including weak mechanical properties, poor processibility, rapid degradation rate and potential immunogenic properties. Thus, the fabrication of polyblend nanofibers by blending two or multiple polymers has been recognized as a powerful approach to maximize the advantages of each component.[14,114,121] For example, polyblend approach enables to integrate the advantages of different types of materials into a new material, thus providing enhanced mechanical strength, bioactivity and degradation profile.

2.3 Surface modification and crosslinking of nanofibers

Surface modification provides a robust approach to improve the physicochemical and biological properties of nanofibers. Several different techniques have been proposed for surface modification of nanofibers by increasing the hydrophilicity and introducing active sites for further biomolecules immobilization, including physical adsorption and coating, plasma modification, wet chemical methods and surface graft polymerization. To construct a more cell-friendly surface, various biomolecules with specific bioactive moieties can be physically absorbed or chemically bonded to the surface of polymer nanofibers without affecting bulk properties. Such biologically functionalized nanofibers possess optimized surface hydrophilicity and chemical compositions, thus providing a more favorable environment for cell growth and tissue regeneration.

2.3.1 Physical absorption. Physical absorption is a simplest technique to immobilize biomolecules onto the nanofiber surfaces, which is driven by non-covalent interactions such as Van der Waals force, electrostatic forces, hydrophobic interactions and hydrogen bonding.[9] However, the immobilization strength and efficiency of biomolecules is relatively weak by direct physical coating.[122] To circumvent this limitation, plasma modification is commonly applied to increase the efficiency of physical absorption onto hydrophobic nanofiber scaffolds by creating a more hydrophilic surface. Plasma-treated polymer nanofibers could enhance cell attachment and migration because of the large quantity of hydrophilic amine and carboxyl surface groups.[123] Furthermore, several types of ECM protein components such as collagen,[124] gelatin,[125,126] laminin[127] and fibronectin[128] can be subsequently immobilized onto the plasma treated nanofibrous surface for enhanced cell function. Other biomolecules such as heparin[129-131] and the mussel-inspired protein poly(dopamine) (PDA)[132-134] can be also introduced to the nanofibrous scaffolds for enhanced anticoagulant and surface adhesion properties.

Layer-by-layer (LbL) assembly is another versatile surface modification approach that typically utilizes electrostatic attraction to assemble polyelectrolyte multilayers (PEM) onto a substratum, allowing nanoscale control over composition and structure.[135-137] This technique has recently been utilized for the surface modification of nanofibrous scaffolds due to the ease of the film assembly and the ability to manipulate the physicochemical, mechanical and biological properties of the coating. For example, PEM containing poly(diallyldimethylammonium chloride) (PDADMAC) and poly(sodium 4-styrene sulfonate) (PSS) can be coated onto the surface of PCL nanofibrous mats by using a LbL self-assembly approach, the coated nanofibers exhibited better mechanical stability and enhanced adhesion and proliferation of fibroblasts than their uncoated counterparts.[138]

2.3.2 Chemical bonding. In contrast to physical absorption, chemical bonding provides a more efficient method for long term preservation of biomolecules. To ensure effective immobilization of bioactive compounds, the appropriate chemical modification should be undertaken to introduce reactive functional groups prior to chemical bonding. Carboxyl and amine groups are the most widely used functional groups for surface modification of polymer nanofiber, which can be introduced to the surface of nanofibrous films by hydrolysis reaction using mild solutions of bases and acids, respectively. For example, carboxyl groups can be exposed on the surface of several polyester nanofibers after treating with alkaline aqueous solution.[139,140] In addition, amine groups can also be grafted onto the surface of polyester nanofibers[128] or be incorporated into the bulk material of nanofibers during the fabrication.[141,142] After activation of these surface reactive groups, biomolecules can be immobilized onto the nanofiber surface, majorly by means of N-(3-Dimethylaminopropyl)-N′-ethylcarbodiimide hydrochloride/N-hydroxysuccinimide (EDC/NHS) chemistry. A variety of bioactive molecules such as ECM proteins, ECM-derived peptides, antibody and heparin have been covalently bonded to the surface of polymer nanofibrous scaffolds to meet various specific requirements in tissue engineering and drug delivery. For example, collagen, one kind of ECM protein, was immobilized onto the nanofiber surface through EDC/NHS chemistry.[143] The collagen-modified nanofibers showed enhanced the attachment and viability of the neural stem cells. In another studies, several specific cell adhesive RGD sequences such as Gly-Arg-Gly-Asp-Ser (GRGDS)[144,145] and Gly-Arg-Gly-Asp-Tyr (GRGDY),[142] can be covalently attached to the surface of polyester nanofibers, resulting in specific cell/material interaction while reducing protein adsorption. Recently, Zhang et al.[146] suggested a convenient approach for achieving stable

hydrophilic surfaces where PCL nanofibers were firstly modified with a class II hydrophobin (HFBI), and the second protein layer of anti-CD31 antibody was subsequently immobilized on the HFBI surface through protein-protein interactions. The resultant PCL scaffolds showed dramatic enhancement in specific binding of human umbilical vein endothelial cells (HUVECs), thus allowing rapid endothelialization on the vascular grafts surface. In addition, heparin is now commonly bonded to the external surface of the nanofibrous scaffolds by EDC chemistry for enhanced cell infiltration[129] or for subsequent growth factors loading.[147]

2.3.3 Crosslinking of nanofibers. Natural nanofibers, fabricated either by electrospinning or self-assembly, generally possess poor mechanical properties and water stability, which limit their use in tissue engineering and drug delivery. To overcome these limitations, crosslinking via either physical or chemical methods is a useful way for improving the mechanical and degradation properties of polymer nanofibers for tissue engineering applications.[148,149]

Chemical crosslinking is a highly versatile method to create nanofibers with good mechanical stability and water-resistant ability, where the commonly used crosslinkers are glutaraldehyde and EDC/NHS chemistries. These crosslinking methods have been largely employed for crosslinking of protein and polysaccharide nanofibers, such as collagen,[150,151] elastin,[152] gelatin,[153-156] fibrinogen,[157] silk fibroin,[158] chitosan[159,160] and cellulose.[161] However, glutaraldehyde treated materials can be cytotoxic[162,163] and induce some side effects *in vivo*, such as calcification and infection.[164,165] Although the crosslinking processes with EDC/NHS chemistries were proven to be nontoxic, the crosslinked nanofibers might lose their stability in aqueous solution.[155,166] To this end, several natural plant crosslinkers including genipin,[154,167] phytic acid[168] and procyanidins[169] have been developed for crosslinking nanofibers. Genipin is an aglycone derived from the fruit of Gardenia jasminoides Ellis, obtained via enzymatic hydrolysis with β-glucosidase.[170] It participates in both short- and long-range covalent cross-linking of ε-amino groups in amine-containing polymers,[171] and can react with amino acid or proteins to form blue pigments that are used in Chinese medicine and the production of food dyes.[172,173] Furthermore, genipin exhibits good biocompatibility and negligible toxicity, making it one of the most widely used crosslinking agent for biomaterials.[174] Due to the ability to covalently bind with the free amine groups on the surface of nanofibers, genipin has recently been utilized for fixing collagen,[175] gelatin,[167] chitosan[176] and silk fibroin[177,178] nanofibrous scaffolds with very minimal cytotoxic effects compared to studies performed with glutaraldehyde. In a recent study, anothor natural plant crosslinker, phytic acid, was applied to crosslink the hemoglobin/gelatin/fibrinogen composite nanofibers for the regeneration of ischemic myocardium.[168] The *in vitro* results showed that the phytic acid-crosslinked scaffold had a significantly higher cell proliferation than glutarladehyde-crosslinked scaffold. In addition, procyanidin was also used for crosslinking of bacterial cellulose/gelatin composite nanofibers, and *in vitro* culture of fibroblasts on the crosslinked scaffold demonstrated good cell viability and a normal cell morphology.[179]

To achieve an effective chemical crosslinking, the polymers must contain specific functional groups which can participate in crosslinking reactions. Therefore, it is difficult to crosslink a polymer without such functional groups. Physical crosslinking such as dehydrothermal treatment (DHT), plasma treatment, gamma or electron beam irradiation, and ultraviolet (UV) treatment can be used as alternative approaches. However, the single use of the physical treatment generally produces a low crosslinking degree because the reaction occurs only at the surface of the materials. Compared with physical crosslinking alone, the combination of physical and chemical crosslinking resulted in a significantly higher crosslinking degree because the crosslinking simultaneously occur in both the surface and the bulk of the nanofibers.[149] Most recently, Lin et al.[148] reported an *in situ* UV-crosslinking method for crosslinking of gelatin electrospun fibers. The UV-crosslinked nanofibers possessed good water-resistant ability with improved mechanical strength. Moreover, they exhibited better biocompatibility for fibroblasts than the glutaraldehyde-crosslinked ones. In another study,[180] a similar *in situ* method was also applied to fabricate polyurethane (PU)/Poly(ethylene glycol) methacrylate (PEGMA) crosslinked scaffolds for vascular tissue engineering application. In order to obtain better thermal stability and mechanical properties of PLLA nanofibers, He et al.[181] recently suggested a gamma radiation-induced crosslinking method in which trially isocyanurate (TAIC) was incorporated into PLLA nanofibers and then crosslinked by gamma radiation at different doses. The effective crosslinking networks can be formed at the appropriate TAIC content and radiation dose. Moreover, the crosslinked PLLA nanofibers were demonstrated to be noncytotoxic and capable of serving as scaffolds for tissue engineering.

3. Biomimetic nanofibers for drug delivery

3.1 Drug-loaded nanofibers

Over the last decade, various kinds of nanofiber-based drug delivery systems have been investigated for delivery of a broad spectrum of bioactive compounds, including therapeutic drugs, proteins,[91] growth factors,[182] genes[183] and even living cells.[184,185] Electrospun nanofiber has been regarded as the most suitable candidate for this purpose, mainly due to its unique functionality and broad selection of building materials. Depending on the polymer carrier and fabrication method used, the eluting profiles of bioactive compounds can be designed as rapid, immediate and delayed manner.[26,27] Currently, bioactive molecules can be formulated within the bulk phase of electrospun nanofibers or on their surface by using different ways, including post treatment of nanofibers (Fig. 6a), immobilization of drug-loaded nanocarriers to nanofibers (Fig. 6b), co-electrospinning of drug/polymer blends (Fig. 6c), coaxial electrospinning and emulsion electrospinning (Fig. 6d). Among these, co-electrospinning is the most popular drug-incorporated method due to its simple process and cheap equipment. The early phase of these studies mainly focused on the encapsulation of various therapeutic drugs within the electrospun nanofibers, with the purpose of developing localized drug delivery system for antibacterial and antitumor therapy. A variety of antibiotics such as tetracycline hydrochloride,[186] mefoxin,[187] ibuprofen,[188] cefazolin,[189] rifampin,[190] Itraconazole,[191] rapamycin[192] and antitumor drugs

such as carmustine,[193] paclitaxel,[190] doxorubicin hydrochloride (DOX),[194-197] cisplatin,[198] 5-fluorouracil,[199] polyphenol[200] and camptothecin[201] have been incorporated into a broad range of electrospun fibers, by fine tuning drug-polymer interactions. However, only a few studies[182,202-205] have involved the incorporation and release of proteins and growth factors from electrospun polymer fibers. Although many studies[206] have demonstrated that the entrapped drugs can maintain their structural integrity and physiological activity, these systems still retain certain limitations. For example, Kim et al.[206] investigated the release of cefoxitin sodium from electrospun poly(lactide-coglycolide) (PLGA) nanofibers. *In vitro* release studies demonstrated that the incorporation of the amphiphilic copolymer PEG-b-PLA into polymer matrix decreased the initial burst drug release and provided a sustained drug release over 1 week. Therefore, the authors proposed that the majority of the drug molecules were primarily located at the fiber surface owing to their high ionic strength in solution and the limited drug-polymer interactions during electrospinning, thus resulting in an initial drug burst release. A more severe problem for some bioactive molecules such as growth factors is their loss of bioactivity upon exposure to harsh solvents. To address these problems, several nanoscale carriers including mesoporous silica nanoparticles (MSNs),[207] halloysite nanotubes[208] and nano hydroxyapatite (HAp)[194] have been entrapped into electrospun nanofibers or immobilized on the surface of nanofibers for the prolonged delivery of therapeutic drugs. In a recent study,[207] an anticancer drug (DOX) was encapsulated into the MSN carriers and the DOX-loaded MSNs were then incorporated in PLLA nanofibers via electrospinning. Thus prepared PLLA composite nanofibers were used as implantable local drug delivery scaffolds for postsurgical cancer treatment and showed higher *in vitro* antitumor efficacy than their MSNs-free counterparts. The authors suggested that incorporation of drugs into MSNs can provide effective protection of the encapsulated drugs against harmful solvents and electric field in the electrospinning process. In order to achieve the desired sustained release profile and ensure a complete package of bioactive molecules within nanofibers, both coaxial and emulsion elctrospinning techniques have been developed for the fabrication of core-sheath nanofibers. In such ways, drugs or bioactive molecules can be enclosed within the polymer shell to form a reservoir-type drug delivery device, within which polymer shell can provide a temporal protection for drug molecules and thus facilitate a controlled drug release.[27,209,210] Huang et al.[27] entrapped resveratrol and gentamycin sulfate in the core of the biodegradable PCL nanofibers through co-axial electrospinning. The release of the drugs from the core was mediated by the biological degradation of PCL by Pseudomonas lipase. The release profiles of both drugs exhibited a sustained release characteristic without burst release phenomenon. He et al.[13] compared the release behavior of two tetracycline hydrochloride-loaded PLLA nanofibers prepared using blend and coaxial electrospinning. The results showed that the blend fibers still produced an initial burst release, while the threads made of core-sheath fibers provided a sustained drug release. Coaxial electrospinning has been ranked as the most popular approach to produce core-sheath fibers for delivery of sensitive bioactive molecules, with the potential beneficial of suppressing burst release and providing protection for the incorporated drugs. Different types of proteins have been successfully encapsulated into coaxially electrospun scaffolds and exhibited efficient bioactivity to regulate corresponding cell behaviors, including BSA,[210,211] lysozyme,[210] vascular endothelial growth factor (VEGF),[212,213] platelet-derived growth factor-bb (PDGF-bb)[214,215] and fibroblast growth factor (FGF).[216] Emulsion electrospinning is a relatively simple technique than coaxial electrospinning.[217,218] However, it requires two immiscible spinning solutions simultaneously. Moreover, some procedures involved in the preparation of protein emulsions such as mechanical stirring, homogenization or ultrasonication, can damage the structure and function of protein molecules.[219] These disadvantages limit its widespread applications.

Another strategy for biomolecules delivery can be achieved by integrating some separate microcarrier systems such as microspheres into nanofibrous scaffolds, where an interconnected macroporous structure is perfected (Fig. 6b). Nanofibrous scaffolds fabricated by TIPS technique commonly require freezing gelation and solvent exchanging process, upon which biomolecules may lose their bioactivity due to harsh environment. Therefore, integrating additional release systems into such scaffolds is desirable to impart scaffolds with drug delivery. In this sense, various growth factors were first incorporated into PLGA microspheres using a double emulsion technique,[220,221] and the medicated microspheres were subsequently attached onto the pore wall surface. The release profiles of biomolecules from such scaffolds are predominantly determined by the intrinsic properties of microspheres.

3.2 Release kinetics of drug-loaded nanofibers

Over the past decade, extensive studies have been conducted to examine the effects of different nanofibers-based pharmaceutical formulations on their release kinetics, and particularly in the arena of the electrospun nanofibers. The researchers have identified several factors that can affect the drug release from electrospun fibers, which mainly include nature of the polymer nanofibers,[186,222,223] fiber geometry,[224] properties of drug,[223,225-227] initial drug loading[222,227] and drug-matrix interaction.[204,228] The release profiles of nanofibers-based drug delivery systems are highly influenced by the state of the drug and the structure of the polymer. Drug release from semi-crystalline polymer nanofibers exhibits a rapid burst release and a subsequent relatively slower sustained release.[186] The crystalline state of incorporated drug in the fibers is also an important factor. For example, high crystalline drugs tend to move onto the surface of fibers during electrospinning and trigger burst release, while drug in amorphous state can be easily encapsulated inside of the fibers and be released in a sustained manner.[226,229,230] The amount of drug loading can also affect the drug release rate, and a higher initial drug loading can result in a faster drug release.[222,227,229] Moreover, the compatibility of drug and polymer solution as well as the interaction between drug and the polymer is also important factors determining the drug release kinetics in nanofibers-based drug delivery system.[225,228] These results and findings obtained from the experimental studies provide important insights for designing nanofibers-based drug delivery system. However, it is desirable to use mathematical models of drug release to predict release kinetics and to better understand the mechanisms controlling drug release from these advanced delivery systems.[2]

In a controlled drug delivery system, drug can be released following three main mechanisms: diffusion, chemical reaction and solvent activation.[231] Most of the current nanofibers-based drug delivery systems are classified as diffusion-controlled system, which can be divided into matrix-type system and reservoir-type system. In a matrix type device, such as

electrospun polyblend nanofibers, the drug is homogeneously distributed into the polymeric matrix. On the other hand, in reservoir type device, such as coaxially electrospun nanofibers, drug core is surrounded by a polymer shell and thus form a core-sheath structure.[196] Generally, a matrix device is easy to provide diffusion-mediated biphasic drug release consisting of a burst release followed by a slow controlled release, while a reservoir device allows a constant and prolonged release of the included drugs.[232] Furthermore, depending on the polymer degradation characteristics, each of the two delivery systems can be surface erosion type where degradation occurs only at the surface or bulk erosion type where degradation takes place throughout the whole body of the polymer matrix. So far, a number of mathematical models have been used to describe drug release profiles from electrospun nanofibrous matrices, such as zero order model,[233,234] first order model,[233,234] Higuchi equation,[233-235] particle diffusion model,[233] Hixon-Crowell model[234] and power law equation (Korsmeyer-Peppas equation).[234-236] Among these models, the simple and more widely used model is the so-called power law equation (or Korsmeyer-Peppas equation) and is as follows:

$$M_t / M_\infty = K t^n$$

where M_t is the accumulative amount of drug released at time t, M_∞ is the initial drug loading, K is a constant characteristic of the drug-polymer system, and n is the diffusion exponent suggesting the nature of release mechanism. As mentioned previously, however, drug release kinetics may be affected by many factors such as polymer swelling and erosion behavior, the drug dissolution and diffusion characteristics, drug distribution in the polymer matrix, drug/polymer ratio and system geometry (slab, cylinder and so on). None of the existing single model can fully describe the whole kinetics of release.[2] Consequently, further efforts should be addressed to develop advanced mathematical models suitable for various nanofibers-based drug delivery systems.

4. Biomimetic nanofibers for tissue engineering

Although various nanofibrous matrices have been applied to almost all the areas of tissue engineering as both scaffolds and carriers for bioactive molecules, this section will focus on a sample of recent applications in the areas of bone, vascular and neural tissue engineering, which represent the active application areas of the above-mentioned three main nanofiber fabrication techniques.

4.1 Bone tissue engineering

The treatment of bone defect with biomimetic nanofiber scaffolds has received significant progress in recent years.[11,237] Natural bone ECM is a type of complex inorganic-organic nanocomposite, in which inorganic HAp and organic collagen fibers are well organized in a multilevel hierarchical architecture.[6,238] These ECM components play important roles in maintaining bone structure and strength. Thus, polymeric nanofibers can be uniquely designed to mimic the components and architecture of bone ECM.[239]

The osteogenic potential of various single component nanofibers has been demonstrated by several *in vitro* and *in vivo* studies. Electrospun PCL scaffold was first applied as a nanofibrous matrix for the bone regeneration, which showed good support for the differentiation of rat bone marrow stromal cells (BMSCs) and *in vitro* calcium phosphate mineralization and collagen deposition.[240] The *in vivo* osteogenic ability of the PCL nanofibrous scaffold was also evaluated by implanting mesenchymal stem cells (MSCs)-seeded scaffolds in the omenta of rats for 4 weeks. MSCs cultured in such a scaffold showed the desired osteogenic differentiation ability and *in vivo* ECM production.[241] To improve the cell compatibility of nanofibrous scaffolds, a variety of polyblend nanofibers consisting of natural and synthetic polymers were developed by either blending[242,243] or coating[125,244] procedures and used as scaffolds for the bone regeneration, which showed good initial adhesion and growth of the different osteogenic cells.

Although some success has been achieved, these polymeric nanofibrous scaffolds may lack adequate osteoconductive ability due to absence of inorganic mineral component. Thus, it is of great importance to fabricate a nanofibrous scaffold comprising a biodegradable polymer and calcium phosphate ceramic for bone regeneration, which not only provides enhanced mechanical properties, but also possesses distinct bioactivity and osteoconductive properties. The most popular approach and easy way to fabricate ceramic/polymer fibrous composites is *in situ* electrospinning of the ceramic and polymer mixture solution. This has led to numerous ceramic-filled polymeric fibrous structures.[245-248] However, due to the incompatibility between ceramic particles and polymeric matrix, this approach usually resulted in uneven distribution of ceramic particles within the polymeric matrix and poor loading capacity of ceramic component, which thereby causes insufficient mechanical strength and poor bioactivity of the composite matrix.[245,249] One of the most common method to create a calcium phosphate coating on the surface of polymer nanofibers is immersing them in simulated body fluid (SBF), which has ion concentrations similar to that of human blood plasma.[250,251] This method allows forming bone-like apatite on the surface of nanofibers, resembling the natural bone mineral phase in composition and structure, and therefore is regarded as the most effective method of creating a biomimetic coating on scaffolds. This method has been adopted to mineralize different types of electrospun nanofibers[140,252-254] and phase-separated nanofibers,[51,57] and some *in vitro* studies demonstrated that the mineralized scaffolds possessed significantly higher bioactivity than the non-mineralized scaffolds.[253,254] However, this is generally a time-consuming process that takes even several weeks to form a homogenous mineral coating on scaffold,[51,140,255] which would probably result in the degradation of polymer materials prior to their clinical applications. Mineralization time can be shortened by using several different methods, including alkaline erosion,[139] plasma treatment[252] and surface functionalization,[253,256] wherein the mineralization can be accelerated by activating and introducing some active functional groups on scaffold surface that are responsibility for apatite mineralization, such as carboxyl, amino and hydroxyl groups. Recently, He et al.[257-259] developed an electrodeposition process in which mineralization can be rapidly completed on different polymer substrates. Compared with SBF incubation, electrodeposition reduced the mineralization time from about two weeks to an hour for deposition the same amounts of calcium phosphates on the PLLA electrospun fibrous matrices (Fig. 7). The mineralization rate also varied with the fiber diameter but in opposite directions between both mineralization methods. The increase of fiber diameter produced a faster mineralization rate for the electrodeposition method but a slower mineralization rate for the SBF incubation. The electrodeposition process tended to form a calcium phosphate layer on the surface of a nanofibrous matrix (Fig. 7c and d). Depending on the deposition potential and electrolyte temperature, the chemical composition and morphology of the calcium phosphate can be custom-made

within a mixture of dicalcium phosphate dehydrate (DCPD) and HAp. In contrast, the SBF process resulted in core-shell mineralized fibers where low-crystallinity HAp crystals were deposited around the individual nanofibers (Fig. 7a and b). Based on these results, the authors suggested the possible deposition mechanisms involved in the two methods. The mineralized PLLA fibrous matrices from either method were found to similarly promote the proliferation and osteogenic differentiation of preosteoblastic MC3T3-E1 cells as compared to neat PLLA matrices. Therefore, the electrodeposition method can be utilized as a fast and versatile technique to fabricate mineralized scaffolds for bone tissue engineering.[257] Moreover, the versatility of electrodeposition method has been demonstrated by the rapid deposition of calcium phosphate on electrospun and phase-separated PLLA fibrous matrices and 3D porous gelatin scaffolds.[257-259]

Osteogenic growth factors and related genes have been incorporated into nanofiber-based scaffolds for enhanced and accelerated bone regeneration. To create an osteoinductive environment, bone morphogenetic protein 2 (BMP-2) was encapsulated directly into silk fibroin/PEO/HAp electrospun nanofibers. The sustained release of BMP resulted in an enhanced osteogenic differentiation of mesenchymal stem cell and calcium deposition.[182] For gene therapy, BMP-2 and plasmid DNA was pre-loaded within chitosan particles and then encapsulated into the PLGA/HAp electrospun scaffold.[260] The composite scaffold showed higher cell viability and more desirable transfection efficiency than other scaffolds in which DNA was only adsorbed on the surface of nanofibers. Using an additional microsphere delivery system, bone morphogenetic protein 7 (BMP-7) and PDGF can be separately incorporated into phase-separated nanofibrous scaffolds for stimulating osteogenesis and angiogenesis *in vivo*.[261-263] Wei et al.[261] reported that BMP-7-loaded PLGA nanospheres could be readily immobilized on the nanofibers of a phase-separated nanofibrous scaffold without blocking interpore connections. After implantation into rats for 3 weeks, the scaffolds soaked with BMP-7 revealed only fibrous tissue formation, whereas scaffolds containing BMP-7 nanospheres showed initial bone formation.

4.2 Vascular tissue engineering

Cardiovascular diseases are still a major cause of mortality and morbidity worldwide. The development of tissue-engineered vascular grafts, especially those of small diameters (inner diameter < 6 mm), is of particular importance for patients who lack sufficient autologous vessels for surgery. To engineer vascular grafts, nanofiber-based strategies have been employed to create vascular grafts with nanoscale structural features. A clinically useful vascular graft should have a confluent endothelium to prevent thrombosis, a biocompatible component with high tensile strength to provide mechanical support, as well as an elastic component to provide recoil and prevent aneurysm formation.[264,265]

Electrospinning has become the most convenience approach to fabricate tubular scaffolds by using a rotating collector and various natural polymers, synthetic polymers and their combination. In this procedure, the fiber composition, size and alignment as well as the scaffold geometry can be fine-tuned for a more efficient vascular cell attachment and spreading.[106,266-270] Using a disk collector, Xu et al.[35] fabricated Poly (L-lactide-co-ε-caprolactone) (PLCL)) nanofibrous scaffold with an aligned nanofibers configuration that imitates the medial layer of native artery. The aligned nanofibrous scaffold was found to have a higher adhesion and proliferation rate of smooth muscle cells (SMCs) than controls. Cytoskeleton proteins were observed to arrange parallel to the alignment direction of the nanofibers, and the SMCs migrated along the axis of nanofibers and acquired a contractile phenotype. To create more biomimetic microenvironments for vascular regeneration, various bi-layered or multilayered tubular scaffolds were developed by combining different materials and techniques.[271-275] To mimic the morphological and mechanical properties of a blood vessel, Vaz et al.[273] electrospun a bi-layered tubular scaffold consisting of an oriented PLLA outside layer and a randomly oriented PCL inner layer. By adjusting the rotation speed of collector, the fiber orientation between different layers can be tuned to create scaffolds with the desired elasticity. A major limitation for electrospun sacffolds is their inherent small pore size that restricts cellular infiltration. To address this problem, a bilayered vascular graft scaffold were developed by the combination of electrospinning and TIPS techniques, where a highly porous TIPS inner layer served as tunica media and an electrospun outer layer with limited porosity used as tunica adventitia.[271] This bilayered scaffold exhibited artery-like mechanical properties and a rapid and efficient cellularization, which is desirable for vascular applications. In another study, Ju et al.[272] fabricated a bi-layered vascular scaffold using two different sizes of PCL/collagen nanofibers, where the inner layer contained a small fiber diameter of 0.27 mm for EC adhesion, while the outer layer was composed of a large fiber diameter of 4.45 mm for SMC infiltration. The scaffolds showed an optimal mechanical properties and compliance that matched to the native artery. Furthermore, some well-designed vascular scaffolds have been examined using *in vivo* models. Wise et al.[274] electrospun a bi-layered vascular graft comprised a luminal layer of pure synthetic elastin (SE) nanofibers and an outer layer of SE/PCL hybrid nanofibers. The incorporation of SE into scaffolds showed an enhanced vascular compatibility by reducing platelet attachment and increasing endothelialization, and a good suturability and mechanical durability in a rabbit model. Most recently, a bi-layered electrospun scaffold was developed for dual delivery of VEGF and PDGF.[212] In this system, VEGF and PDGF were separately encapsulated into the inner and outer layer of scaffolds by using coaxial and emulsion electrospinning, respectively. After implanted into rabbit carotid artery *in vivo* for 4 weeks, the vascular graft developed into a cellularized tubular construct that the ECs attached on the lumen and SMCs grew on the outer surface. The most promising advance in electrospinning is the direct fabrication of cell-bearing vascular scaffolds either by combining an electrospray technique with electrospinning[276,277] or by applying cell electrospinning technique.[184,278] In these studies, various living vascular cells were *in situ* encapsulated into electrospun fibers to form cell-laden scaffolds under a cell friendly environment. More interestingly, Jayasinghe's group recently reported that living vessel-like architectures could be fabricated with different vascular cell types at different layers by using custom-made cell electrospinning equipment. The encapsulated cells can retain their viability and functionality in the fabricated cell-bearing sheet and 3D vessel-like architecture, and the vessel-like architecture contains the two cores each having a different type of vascular cell (Fig. 8).[184,185] As such, the technique could enable the rapid generation of living vascular grafts, which obviates the need for manual cell seeding and subsequent bioreactor incubation, thus reducing the spatial non-uniformity of the seeded cells and the time required for cell infiltration into the scaffold.[184,185,278]

Phase separation has been used for fabricating nanofiber-based vascular scaffolds.[279-282] With phase separation, it is able to generate a scaffold with pre-defined and precisely controlled macropore structures, which can enable a more efficient scaffold cellularization. Several studies[279,281,282] have demonstrated that the phase-separated PLLA nanofibrous scaffolds could promote the cellular differentiation and vascular tissue infiltration. However, PLLA is a rigid polymer that is unable to provide intrinsic viscoelasticity for vascular graft, which is critical for its long-term patency and overall biological performance. Hence, the mechanical properties are of a major concern for the development of phase-separated vascular grafts. A recent study showed that mechanical properties of the PLLA-based nanofibrous vascular grafts could be greatly improved by phase separating a polymer blend of PLLA and more elastic polymer (such as PLCL). [283]

Self-assembling peptide nanofibers have also been considered promising candidates for vascular tissue engineering applications. Several self-assembled peptide scaffolds, such as RAD16-I and RAD16-II, which contain an RGD-like motif, have been shown to provide an angiogenic environment promoting survival of ECs and angiogenesis both *in vitro* and *in vivo*.[284-287] A recent *in vivo* study suggested that the pro-angiogenic effect of RAD16-II might result from a weak interaction between ECs and RAD peptides, which triggers angiogenic responses via the β3 integrin/MAPK/ERK pathway.[285] Similarly, several self-assembled PA nanofibers containing different cell adhesive sequences have been demonstrated to enhance the adhesion and spreading of vascular cells.[68,288] To mimic the cellular and matrix organization found in native arteries, McClendon et al.[68] recently developed a kind of tubular hydrogel scaffold with circumferential alignment PA nanofibers, which allows for the growth of the 3D encapsulated human SMCs into a living vessel-like tissue containing the circumferentially aligned SMCs layer. The tubular constructs were fabricated in a custom built flow chamber by sequentially shearing the PA solution with suspended SMCs then gelling through exposure to Ca^{2+} ions (Fig. 9a-d). The SEM image indicated that PA nanofibers were well-aligned on the inner surface of the fabricated tube (Fig. 9e). The calcein staining of viable cells revealed that the encapsulated SMCs had good cell viability in tubular construct after 7 days of culture (Fig. 9f). Furthermore, the cross-sectional fluorescence image of F-actin staining showed that almost all cells were aligned in the circumferential direction after 4 days of culture, which resembles histological cross sections of native arterial medial layers (Fig. 9g). Therefore, this technique may be suited for developing the highly organized tissue engineered blood vessels. Additionally, the self-assembled peptide hydrogels could be chemically modified to improve their mechanical properties and enhance the proliferation and phenotypic expression of endothelial cells.[289] Taken together, molecular self-assembly approach opens a new avenue for efficient vascular regeneration and repair. However, the complexity of the self-assembly process, plus the current low productivity limits its practical applications.

4.3 Neural tissue engineering

The regeneration of injured nervous tissues poses a tremendous challenge, especially in the central nervous system (CNS) where neural regeneration is even more complex due to the non-permissive regenerative environment created after injury in the CNS.[290] Tissue engineering approach has become an effective strategy to repair neural defects, which is focused on the development of artificial nerve guidance conduits (NGCs) to overcome the limitations of conventional autologous and allogeneic nerve grafts.[291] An ideal nerve conduit requires a biocompatible, biodegradable, neuroconductive, neuroinductive and mechanically robust 3D porous scaffold, which can be custom engineered to provide the essential biochemical, mechanical, electrical and topographical signals for regulating cell behavior and tissue progression. Nanofibers are intriguing materials for this application due to their structural similarity to the native neural ECM and ability to direct neurite outgrowth.[292]

The feasibility of using electrospun nanofibers for neural regeneration has been demonstrated both *in vitro* and *in vivo* assays. In these applications, nanofibers could be not only fabricated from a multitude of synthetic, natural and combined materials, but also assembled into a variety of scaffolds or conduits with hierarchical structure by manipulating fiber morphology, alignment, stacking and folding.[291] Scaffold properties including material composition, fiber diameters and scaffold porosity have been demonstrated to greatly affect cell behavior and function.[141,293,294] More interestingly, the aligned nanofibers have been shown to provide topographical cues and contact guidance for different types of neural cells, and thus promote cell migration and axonal extension in the designated direction.[294-299] The aligned PLLA nanofibrous scaffolds have been found to be better suited for the growth of C17.2 neural stem cells (NSCs) than non-aligned nanofibrous scaffolds. On the aligned nanofibrous scaffolds, the NSCs were able to sense the anisotropic topography of the underlying scaffold by elongating and neurite outgrowth along the fiber orientation.[298] Similarly, the aligned PCL nanofibers have also been demonstrated to provide contact guidance for human Schwann cells, resulting in that cell cytoskeleton and nuclei aligned and elongated along the fiber axes. Furthermore, the up-regulation of the myelin-specific gene expression only on aligned electrospun fibers suggested that aligned fibers may promote Schwann-cell maturation, which is beneficial for peripheral nerve regeneration.[297] By manipulating electrospun scaffolds with varying orders, structures and surface properties, a recent study has shown that neurite outgrowth can be pronouncedly affected by fiber alignment, architecture and density in the scaffolds (Fig. 10). When embryonic chick dorsal root ganglia (DRG) were cultured on single-layered scaffolds that only contained either randomly oriented or aligned nanofibers (Fig. 10a and c), the neurites were uniformly distributed on scaffolds with random fibers and grew preferentially along the fibers on scaffolds with aligned fibers (Fig. 10b and d). When DRG were cultured at the border between regions of aligned and random nanofibers (Fig. 10e), the same DRG simultaneously expressed aligned and random neurite fields to recognize the topographical cues from the underlying nanofibers (Fig. 10f). However, when DRG were seeded on a bilayered scaffold comprising two layers of perpendicularly aligned nanofibers, the extension of neuritis was regulated in a density dependent manner by the fiber orientation in both layers rather than the surface layer only. At low fiber density (Fig. 10g), some of the neuritis grew initially along the direction of fiber alignment in one layer, but they then extended parallel to the long axis of the fibers in the other layer (Fig. 10h).[300] Furthermore, a more recent study by the same group reported that the direction of DRG neurite growth on uniaxially aligned electrospun nanofibers could be either parallel or perpendicular to the direction of fiber alignment. The direction is determined by various parameters including fiber density, surface chemistry of the fibers and surface property of the supporting substrate.[301] Some *in vivo* studies[302,303] have also suggested that the

scaffolds consisting of aligned nanofibers could enhance nerve regeneration and functional recovery through contact guidance. The efficiency of nerve regeneration could be further improved by incorporating of bioactive molecules such as ECM proteins[304] and growth factors[299,305,306] into electrospun nanofibers. Additionally, several electroconducting polymers such as polypyrrole (PPy) and polyaniline (PANI) have been introduced into electrospun nanofibers to provide electrical signals for directing the neurites and axonal growth *in vitro*.[307-311] PPy-coated PLGA electrospun scaffolds have been found to promote the growth and differentiation of rat pheochromocytoma 12 (PC12) cells and hippocampal neurons than uncoated scaffolds. After electrical stimulated at a potential of 10 mV/cm, PC12 cells cultured on PPy-PLGA scaffolds have been shown to exhibit 40-50% longer neurites and 40-90% more neurite formation compared to unstimulated cells on the same scaffolds. Further study have demonstrated that electrical stimulation of the cells on aligned electrically active fibers resulted in longer neurites and more neurite-bearing cells than stimulation on randomly oriented conductive fibers.[311] In another separate study,[308] conductive PLLA-PPy or PCL-PPy core-sheath nanofibers were fabricated by a combination of electrospinning and *in situ* aqueous polymerization. Two types of aligned conductive nanofibers have shown to be more effective in promoting neurite outgrowth in terms of the length of extended neurites. Consequently, the optimal nerve regeneration and functional recovery would be expected by simultaneously integrating electrical stimulation, topographic cues and biochemical signals into a nanofibrous scaffold.

Self-assembling peptide based materials have also been extensively used in nerve regeneration due to their inherent biocompatibility, the ability to display natural signaling epitopes at controlled densities, and ease of incorporation of cells and growth factors into a nanofibrous gel.[72] By incorporating different bioactive peptide sequences, the self-assembled PAs can be customized to suit specific needs in nerve regeneration.[312] For instance, self-assembled PAs containing a laminin-derived epitope Ile-Lys-Val-Ala-Val (IKVAV) were demonstrated to enhance cell adhesion, proliferation, spreading, migration and neurite outgrowth,[70,313] and selectively promote development of neural progenitor cells into neurons while reduce astrocyte formation and hence minimizing the risk of glial scars.[71] Furthermore, the use of IKVAV PA nanofibers in a mouse model of spinal cord injury (SCI) have shown to reduce astrogliosis and cell apoptosis at the injury site and promote the regeneration of motor and sensory axons.[63] Integration of RGD motifs into self-assembled nanofibers is another popular method that facilitates neural cell growth and tissue regeneration.[314] Additionally, RAD16 self-assembling peptide scaffolds are also considered as promising material for application in both peripheral and central nerve regeneration.[75,81,315-317] By culturing different types of neuronal cells on the RAD16 self-assembling peptide scaffolds, Holmes et al.[75] demonstrated that these peptide scaffolds could support neuronal cell attachment and differentiation as well as extensive neurite outgrowth. Furthermore, these scaffolds could also promote the formation of functional synapses in rat hippocampal neurons. The possibility of using RAD16 peptide scaffolds for treatment of spinal cord injury was also demonstrated in a rat model of spinal cord injury.[317] The neural progenitor cells and Schwann cells were cultured within the nanofibous gels, and then transplanted into the transected dorsal column of spinal cord of rats. After 6 weeks of transplantation, the implants integrated well with the host tissue via host cells migration, blood vessel formation and axons outgrowth within the scaffolds. Therefore, RAD16 peptide scaffold would be a potential material to bridge the injured axons cross the lesion site after spinal cord injury.

5. Conclusion and future prospects

Over the past decade, biomimetic nanofibers have emerged as powerful tools for constructing ECM-mimicking scaffolds to promote tissue regeneration. The nanofibrous scaffolds have proved to be particularly advantageous for cell adhesion and tissue repair due to their unique nanoscale characteristics. Recent advances in nanofiber fabrication techniques have allowed for the development of nanofibrous scaffolds with controllable compositions, structures and surface chemistries. Such nanofibrous scaffolds can also be used as platforms for the delivery of bioactive and therapeutic agents, thus providing beneficial signaling microenvironment to regulate cell growth and tissue regeneration. Relying on different fabrication techniques used, various bioactive compounds can be incorporated within nanofibrous scaffolds by physical adsorption, *in situ* incorporation and covalent immobilization, potentially creating a more biomimetic environment for tissue regeneration. Moreover, the nanofibrous features can be integrated into complex 3-D geometrical scaffolds by combining with other new-emerging technologies like additive manufacturing,[318] which offers opportunities for fine-tuning the scaffold architecture and pore distribution, whilst preserving nanoscale dimensions.

Despite heady progress, several technique hurdles remain to be addressed for moving these promising techniques from bench top to bed side. While a major hurdle encountered in current electrospinning technique is the limited ability to control architectural properties such as pore size and porosity of the scaffolds, which probably leads to poor cell infiltration and the failure in tissue engineering, the limitations of molecular self-assembly and phase separation techniques are the low productivity, relatively narrow range of work materials and high costs. Additionally, current knowledge on the role of the material composition, fiber arrangement, structural geometry, surface properties and release profiles of various nanofibrous scaffolds in the modulation of cellular responses and tissue morphogenesis is still incomplete. A thorough understanding of cell-nanofibrous matrix interactions would yield better design of biomimetic nanofibrous scaffold for tissue engineering applications. Improvement of existing techniques and combination of novel techniques in the nanofiber fabrication area would greatly accelerate the progress in the burgeoning field of tissue engineering.

Acknowledgements

This work was financially supported by the National Natural Science Foundation of China (No. 31271028, No. 51203021) and the Innovation Program of Shanghai Municipal Education Commission (No. 13ZZ051).

Notes and references

Corresponding author at: College of Chemistry, Chemical Engineering and Biotechnology, Donghua University, Shanghai, 201620. Tel./fax: +86 21 67792742. Email address: hcl@dhu.edu.cn (C. L. He)

1 T. Dvir, B. P. Timko, D. S. Kohane and R. Langer, *Nat. Nanotechnol.*, 2011, **6**, 13-22.

2 W. Ji, Y. Sun, F. Yang, J. van den Beucken, M. W. Fan, Z. Chen and J. A. Jansen, *Pharm. Res.*, 2011, **28**, 1259-1272.
3 M. P. Lutolf and J. A. Hubbell, *Nat. Biotechnol.*, 2005, **23**, 47-55.
4 X. F. Wang, B. Ding and B. Y. Li, *Mater. Today*, 2013, **16**, 229-241.
5 R. J. Wade and J. A. Burdick, *Mater. Today*, 2012, **15**, 454-459.
6 M. M. Stevens and J. H. George, *Science*, 2005, **310**, 1135-1138.
7 G. D. Prestwich, *J. Cell. Biochem.*, 2007, **101**, 1370-1383.
8 Y. C. Toh, S. Ng, Y. M. Khong, X. Zhang, Y. J. Zhu, P. C. Lin, C. M. Te, W. X. Sun and H. R. Yu, *Nano Today*, 2006, **1**, 34-43.
9 V. Beachley and X. J. Wen, *Prog. Polym. Sci.*, 2010, **35**, 868-892.
10 Z. M. Huang, Y. Z. Zhang, M. Kotaki and S. Ramakrishna, *Compos. Sci. Technol.*, 2003, **63**, 2223-2253.
11 Z. P. Zhang, J. Hu and P. X. Ma, *Adv. Drug Delivery Rev.*, 2012, **64**, 1129-1141.
12 S. G. Zhang, *Nat. Biotechnol.*, 2003, **21**, 1171-1178.
13 C. L. He, Z. M. Huang and X. J. Han, *J. Biomed. Mater. Res., Part A*, 2009, **89A**, 80-95.
14 J. Gunn and M. Q. Zhang, *Trends Biotechnol.*, 2010, **28**, 189-197.
15 P. X. Ma, *Adv. Drug Delivery Rev.*, 2008, **60**, 184-198.
16 J. D. Hartgerink, E. Beniash and S. I. Stupp, *Science*, 2001, **294**, 1684-1688.
17 A. Greiner and J. H. Wendorff, *Angew. Chem., Int. Ed.*, 2007, **46**, 5670-5703.
18 D. Li and Y. N. Xia, *Adv. Mater.*, 2004, **16**, 1151-1170.
19 Y. F. Qian, Y. Su, X. Q. Li, H. S. Wang and C. L. He, *Iran. Polym. J.*, 2010, **19**, 123-129.
20 D. H. Reneker and I. Chun, *Nanotechnology*, 1996, **7**, 216-223.
21 B. M. Baker, A. O. Gee, R. B. Metter, A. S. Nathan, R. A. Marklein, J. A. Burdick and R. L. Mauck, *Biomaterials*, 2008, **29**, 2348-2358.
22 B. Ding, E. Kimura, T. Sato, S. Fujita and S. Shiratori, *Polymer*, 2004, **45**, 1895-1902.
23 S. Kidoaki, I. K. Kwon and T. Matsuda, *Biomaterials*, 2005, **26**, 37-46.
24 Z. C. Sun, E. Zussman, A. L. Yarin, J. H. Wendorff and A. Greiner, *Adv. Mater.*, 2003, **15**, 1929-1932.
25 D. Li and Y. N. Xia, *Nano Lett.*, 2004, **4**, 933-938.
26 C. L. He, Z. M. Huang, X. J. Han, L. Liu, H. S. Zhang and L. S. Chen, *J. Macromol. Sci., Part B: Phys.*, 2006, **45**, 515-524.
27 Z. M. Huang, C. L. He, A. Z. Yang, Y. Z. Zhang, X. J. Hang, J. L. Yin and Q. S. Wu, *J. Biomed. Mater. Res., Part A*, 2006, **77A**, 169-179.
28 R. R. Yang, J. H. He, L. Xu and J. Y. Yu, *Polymer*, 2009, **50**, 5846-5850.
29 H. T. Niu and T. Lin, *J. Nanomater.*, 2012, **2012**, 725950.
30 D. Li, T. Wu, N. He, J. Wang, W. Chen, L. He, C. Huang, H. A. EI-Hamshary, S. S. Al-Deyab and Q. Ke, *Colloids Surf., B*, 2014, **121**, 432-443.
31 H. Pan, L. M. Li, L. Hu and X. J. Cui, *Polymer*, 2006, **47**, 4901-4904.
32 W. Hu, Z. M. Huang, S. Y. Meng and C. L. He, *J. Mater. Sci.: Mater. Med.*, 2009, **20**, 2275-2284.
33 A. Theron, E. Zussman and A. L. Yarin, *Nanotechnology*, 2001, **12**, 384-390.
34 P. Katta, M. Alessandro, R. D. Ramsier and G. G. Chase, *Nano Lett.*, 2004, **4**, 2215-2218.
35 C. Y. Xu, R. Inai, M. Kotaki and S. Ramakrishna, *Biomaterials*, 2004, **25**, 877-886.
36 D. Li, Y. L. Wang and Y. N. Xia, *Adv. Mater.*, 2004, **16**, 361-366.
37 D. Li, Y. L. Wang and Y. N. Xia, *Nano Lett.*, 2003, **3**, 1167-1171.
38 J. L. Wu, C. Huang, W. Liu, A. L. Yin, W. M. Chen, C. L. He, H. S. Wang, S. Liu, C. Y. Fan, G. L. Bowlin and X. M. Mo, *J. Biomed. Nanotechnol.*, 2014, **10**, 603-614.
39 J. L. Wu, S. Liu, L. P. He, H. S. Wang, C. L. He, C. Y. Fan and X. M. Mo, *Mater. Lett.*, 2012, **89**, 146-149.
40 M. S. Khil, S. R. Bhattarai, H. Y. Kim, S. Z. Kim and K. H. Lee, *J. Biomed. Mater. Res., Part B*, 2005, **72B**, 117-124.
41 D. M. Zhang and J. Chang, *Nano Lett.*, 2008, **8**, 3283-3287.
42 H. Li, Y. Xu, H. Xu and J. Chang, *J. Mater. Chem. B*, 2014, **2**, 5492-5510.
43 D. M. Zhang and J. Chang, *Adv. Mater.*, 2007, **19**, 3664-3667.
44 G. B. Wei and P. X. Ma, *J. Biomed. Mater. Res., Part A*, 2006, **78A**, 306-315.
45 X. H. Liu and P. X. Ma, *Biomaterials*, 2009, **30**, 4094-4103.
46 R. Y. Zhang and P. X. Ma, *J. Biomed. Mater. Res.*, 2000, **52**, 430-438.
47 V. J. Chen and P. X. Ma, *Biomaterials*, 2004, **25**, 2065-2073.
48 L. M. He, Y. Q. Zhang, X. Zeng, D. P. Quan, S. Liao, Y. S. Zeng, J. Lu and S. Ramakrishna, *Polymer*, 2009, **50**, 4128-4138.
49 G. B. Wei and P. X. Ma, *Adv. Funct. Mater.*, 2008, **18**, 3568-3582.
50 X. H. Liu, Y. J. Won and P. X. Ma, *Biomaterials*, 2006, **27**, 3980-3987.
51 R. Y. Zhang and P. X. Ma, *J. Biomed. Mater. Res.*, 1999, **45**, 285-293.
52 P. X. Ma and R. Y. Zhang, *J. Biomed. Mater. Res.*, 1999, **46**, 60-72.
53 L. M. He, B. Liu, X. P. Guan, G. Y. Xie, S. S. Liao, D. P. Quan, D. Z. Cai, J. Lu and S. Ramakrishna, *Eur. Cells Mater.*, 2009, **18**, 63-74.
54 S. Tang, J. X. Zhu, Y. B. Xu, A. P. Xiang, M. H. Jiang and D. P. Quan, *Biomaterials*, 2013, **34**, 7086-7096.
55 X. T. Li, Y. Zhang and G. Q. Chen, *Biomaterials*, 2008, **29**, 3720-3728.
56 J. H. Zhao, W. Q. Han, H. D. Chen, M. Tu, R. Zeng, Y. F. Shi, Z. G. Cha and C. R. Zhou, *Carbohydr. Polym.*, 2011, **83**, 1541-1546.
57 X. Liu, L. A. Smith, J. Hu and P. X. Ma, *Biomaterials*, 2009, **30**, 2252-2258.
58 G. M. Whitesides and M. Boncheva, *Proc. Natl. Acad. Sci. U. S. A.*, 2002, **99**, 4769-4774.
59 D. N. Woolfson and Z. N. Mahmoud, *Chem. Soc. Rev.*, 2010, **39**, 3464-3479.
60 J. D. Hartgerink, E. Beniash and S. I. Stupp, *Proc. Natl. Acad. Sci. U. S. A.*, 2002, **99**, 5133-5138.
61 M. J. Webber, J. Tongers, M. A. Renault, J. G. Roncalli, D. W. Losordo and S. I. Stupp, *Acta Biomater.*, 2010, **6**, 3-11.
62 S. Ghanaati, M. J. Webber, R. E. Unger, C. Orth, J. F. Hulvat, S. E. Kiehna, M. Barbeck, A. Rasic, S. I. Stupp and C. J. Kirkpatrick, *Biomaterials*, 2009, **30**, 6202-6212.
63 V. M. Tysseling-Mattiace, V. Sahni, K. L. Niece, D. Birch, C. Czeisler, M. G. Fehlings, S. I. Stupp and J. A. Kessler, *J. Neurosci.*, 2008, **28**, 3814-3823.
64 H. Z. Jiang, M. O. Guler and S. I. Stupp, *Soft Matter*, 2007, **3**, 454-462.
65 A. Mata, Y. B. Geng, K. J. Henrikson, C. Aparicio, S. R. Stock, R. L. Satcher and S. I. Stupp, *Biomaterials*, 2010, **31**, 6004-6012.
66 M. J. Webber, J. B. Matson, V. K. Tamboli and S. I. Stupp, *Biomaterials*, 2012, **33**, 6823-6832.
67 R. N. Shah, N. A. Shah, M. M. D. Lim, C. Hsieh, G. Nuber and S. I. Stupp, *Proc. Natl. Acad. Sci. U. S. A.*, 2010, **107**, 3293-3298.
68 M. T. McClendon and S. I. Stupp, *Biomaterials*, 2012, **33**, 5713-5722.
69 A. Tan, J. Rajadas and A. M. Seifalian, *J. Controlled Release*, 2012, **163**, 342-352.
70 S. Sur, E. T. Pashuck, M. O. Guler, M. Ito, S. I. Stupp and T. Launey,

Biomaterials, 2012, **33**, 545-555.
71 G. A. Silva, C. Czeisler, K. L. Niece, E. Beniash, D. A. Harrington, J. A. Kessler and S. I. Stupp, *Science*, 2004, **303**, 1352-1355.
72 S. Sur, C. J. Newcomb, M. J. Webber and S. I. Stupp, *Biomaterials*, 2013, **34**, 4749-4757.
73 S. Soukasene, D. J. Toft, T. J. Moyer, H. M. Lu, H. K. Lee, S. M. Standley, V. L. Cryns and S. I. Stupp, *Acs Nano*, 2011, **5**, 9113-9121.
74 J. B. Matson, M. J. Webber, V. K. Tamboli, B. Weber and S. I. Stupp, *Soft Matter*, 2012, **8**, 6689-6692.
75 T. C. Holmes, S. de Lacalle, X. Su, G. S. Liu, A. Rich and S. G. Zhang, *Proc. Natl. Acad. Sci. U. S. A.*, 2000, **97**, 6728-6733.
76 Y. Loo, S. G. Zhang and C. A. E. Hauser, *Biotechnol. Adv.*, 2012, **30**, 593-603.
77 S. G. Zhang, T. C. Holmes, C. M. Dipersio, R. O. Hynes, X. Su and A. Rich, *Biomaterials*, 1995, **16**, 1385-1393.
78 S. G. Zhang, T. Holmes, C. Lockshin and A. Rich, *Proc. Natl. Acad. Sci. U. S. A.*, 1993, **90**, 3334-3338.
79 A. Horii, X. M. Wang, F. Gelain and S. G. Zhang, *Plos One*, 2007, **2**, e190.
80 E. Genove, C. Shen, S. G. Zhang and C. E. Semino, *Biomaterials*, 2005, **26**, 3341-3351.
81 C. E. Semino, J. Kasahara, Y. Hayashi and S. G. Zhang, *Tissue Eng.*, 2004, **10**, 643-655.
82 J. Kisiday, M. Jin, B. Kurz, H. Hung, C. Semino, S. Zhang and A. J. Grodzinsky, *Proc. Natl. Acad. Sci. U. S. A.*, 2002, **99**, 9996-10001.
83 V. Gauba and J. D. Hartgerink, *J. Am. Chem. Soc.*, 2007, **129**, 2683-2690.
84 S. E. Paramonov, H. W. Jun and J. D. Hartgerink, *J. Am. Chem. Soc.*, 2006, **128**, 7291-7298.
85 F. W. Kotch and R. T. Raines, *Proc. Natl. Acad. Sci. U. S. A.*, 2006, **103**, 3028-3033.
86 S. Vieth, C. M. Bellingham, E. W. Keeley, S. M. Hodge and D. Rousseau, *Biopolymers*, 2007, **85**, 199-206.
87 C. M. Bellingham, M. A. Lillie, J. M. Gosline, G. M. Wright, B. C. Starcher, A. J. Bailey, K. A. Woodhouse and F. W. Keeley, *Biopolymers*, 2003, **70**, 445-455.
88 M. Miao, J. T. Cirulis, S. Lee and F. W. Keeley, *Biochemistry*, 2005, **44**, 14367-14375.
89 N. Bhardwaj and S. C. Kundu, *Biotechnol. Adv.*, 2010, **28**, 325-347.
90 W. J. Jin, H. K. Lee, E. H. Jeong, W. H. Park and J. H. Youk, *Macromol. Rapid Commun.*, 2005, **26**, 1903-1907.
91 Y. Z. Zhang, X. Wang, Y. Feng, J. Li, C. T. Lim and S. Ramakrishna, *Biomacromolecules*, 2006, **7**, 1049-1057.
92 X. Q. Li, M. A. Kanjwal, L. Lin and I. S. Chronakis, *Colloids Surf., B*, 2013, **103**, 182-188.
93 S. A. Theron, E. Zussman and A. L. Yarin, *Polymer*, 2004, **45**, 2017-2030.
94 J. M. Deitzel, J. D. Kleinmeyer, J. K. Hirvonen and N. C. B. Tan, *Polymer*, 2001, **42**, 8163-8170.
95 X. Y. Dai, W. Nie, Y. C. Wang, Y. Shen, Y. Li and S. J. Gan, *J. Mater. Sci.: Mater. Med.*, 2012, **23**, 2709-2716.
96 R. R. Klossner, H. A. Queen, A. J. Coughlin and W. E. Krause, *Biomacromolecules*, 2008, **9**, 2947-2953.
97 H. J. Jin, S. V. Fridrikh, G. C. Rutledge and D. L. Kaplan, *Biomacromolecules*, 2002, **3**, 1233-1239.
98 B. Duan, C. H. Dong, X. Y. Yuan and K. D. Yao, *J. Biomater. Sci., Polym. Ed*, 2004, **15**, 797-811.
99 W. I. Park, M. Kang, H. S. Kim and H. J. Jin, *Macromol. Symp.*, 2007, **249**, 289-294.
100 M. Pakravan, M. C. Heuzey and A. Ajji, *Polymer*, 2011, **52**, 4813-4824.
101 J. A. Matthews, G. E. Wnek, D. G. Simpson and G. L. Bowlin, *Biomacromolecules*, 2002, **3**, 232-238.
102 R. Chen, X. Q. Li, Q. F. Ke, C. L. He and X. M. Mo, *e-Polym.*, 2010, 10, 67-74.
103 R. Chen, C. Huang, Q. F. Ke, C. L. He, H. S. Wang and X. M. Mo, *Colloids Surf., B*, 2010, **79**, 315-325.
104 Z. M. Huang, Y. Z. Zhang, S. Ramakrishna and C. T. Lim, *Polymer*, 2004, **45**, 5361-5368.
105 Y. Su, X. Q. Li, S. P. Liu, H. S. Wang and C. L. He, *J. Appl. Polym. Sci.*, 2010, **117**, 542-547.
106 M. Y. Li, M. J. Mondrinos, M. R. Gandhi, F. K. Ko, A. S. Weiss and P. I. Lelkes, *Biomaterials*, 2005, **26**, 5999-6008.
107 K. H. Zhang, X. M. Mo, C. Huang, C. L. He and H. S. Wang, *J. Biomed. Mater. Res., Part A*, 2010, **93A**, 976-983.
108 L. P. Fan, Z. X. Cai, K. H. Zhang, F. Han, J. L. Li, C. L. He, X. M. Mo, X. G. Wang and H. S. Wang, *Colloids Surf., B*, 2014, **117**, 14-20.
109 L. P. Fan, H. S. Wang, K. H. Zhang, C. L. He, Z. X. Cai and X. M. Mo, *J. Biomater. Sci., Polym. Ed*, 2012, **23**, 497-508.
110 L. P. Fan, H. S. Wang, K. H. Zhang, Z. X. Cai, C. L. He, X. Y. Sheng and X. M. Mo, *RSC Adv.*, 2012, **2**, 4110-4119.
111 X. Y. Sheng, L. P. Fan, C. L. He, K. H. Zhang, X. M. Mo and H. S. Wang, *Int. J. Biol. Macromol.*, 2013, **56**, 49-56.
112 C. He, L. Zhang, H. Wang, F. Zhang and X. Mo, *Nano Biomed. Eng.*, 2009, **1**, 80-88.
113 G. E. Wnek, M. E. Carr, D. G. Simpson and G. L. Bowlin, *Nano Lett.*, 2003, **3**, 213-216.
114 C. L. He, X. H. Xu, F. Zhang, L. J. Cao, W. Feng, H. S. Wang and X. M. Mo, *J. Biomed. Mater. Res., Part A*, 2011, **97A**, 339-347.
115 D. Gugutkov, J. Gustavsson, M. P. Ginebra and G. Altankov, *Biomater. Sci.*, 2013, **1**, 1065-1073.
116 Z. G. Chen, P. W. Wang, B. Wei, X. M. Mo and F. Z. Cui, *Acta Biomater.*, 2010, **6**, 372-382.
117 Z. X. Cai, X. M. Mo, K. H. Zhang, L. P. Fan, A. L. Yin, C. L. He and H. S. Wang, *Int. J. Mol. Sci.*, 2010, **11**, 3529-3539.
118 Z. G. Chen, X. M. Mo, C. L. He and H. S. Wang, *Carbohydr. Polym.*, 2008, **72**, 410-418.
119 Y. Ji, K. Ghosh, X. Z. Shu, B. Q. Li, J. C. Sokolov, G. D. Prestwich, R. A. F. Clark and M. H. Rafailovich, *Biomaterials*, 2006, **27**, 3782-3792.
120 C. A. Bonino, K. Efimenko, S. I. Jeong, M. D. Krebs, E. Alsberg and S. A. Khan, *Small*, 2012, **8**, 1928-1936.
121 F. Chen, X. Q. Li, X. M. Mo, C. L. He, H. S. Wang and Y. Ikada, *J. Biomater. Sci., Polym. Ed*, 2008, **19**, 677-691.
122 H. S. Koh, T. Yong, C. K. Chan and S. Ramakrishna, *Biomaterials*, 2008, **29**, 3574-3582.
123 Q. Cheng, B. L. P. Lee, K. Komvopoulos, Z. Q. Yan and S. Li, *Tissue Eng. Part A*, 2013, **19**, 1188-1198.
124 W. He, Z. W. Ma, T. Yong, W. E. Teo and S. Ramakrishna, *Biomaterials*, 2005, **26**, 7606-7615.
125 Z. W. Ma, W. He, T. Yong and S. Ramakrishna, *Tissue Eng.*, 2005, **11**, 1149-1158.
126 J. P. Chen and C. H. Su, *Acta Biomater.*, 2011, **7**, 234-243.
127 N. E. Zander, J. A. Orlicki, A. M. Rawlett and T. P. Beebe, *ACS Appl.*

Mater. Interfaces, 2012, **4**, 2074-2081.
128 Y. B. Zhu, M. F. Leong, W. F. Ong, M. B. Chan-Park and K. S. Chian, *Biomaterials*, 2007, **28**, 861-868.
129 K. T. Kurpinski, J. T. Stephenson, R. R. R. Janairo, H. M. Lee and S. Li, *Biomaterials*, 2010, **31**, 3536-3542.
130 Y. K. Liang and K. L. Kiick, *Acta Biomater.*, 2014, **10**, 1588-1600.
131 S. D. Wang, Y. Z. Zhang, H. W. Wang and Z. H. Dong, *Int. J. Biol. Macromol.*, 2011, **48**, 345-353.
132 J. W. Xie, S. P. Zhong, B. Ma, F. D. Shuler and C. T. Lim, *Acta Biomater.*, 2013, **9**, 5698-5707.
133 S. H. Ku and C. B. Park, *Biomaterials*, 2010, **31**, 9431-9437.
134 N. G. Rim, S. J. Kim, Y. M. Shin, I. Jun, D. W. Lim, J. H. Park and H. Shin, *Colloids Surf., B*, 2012, **91**, 189-197.
135 W. Feng, W. Nie, C. L. He, X. J. Zhou, L. Chen, K. X. Qiu, W. Z. Wang and Z. Q. Yin, *ACS Appl. Mater. Interfaces*, 2014, **6**, 8447-8460.
136 C. Boura, P. Menu, E. Payan, C. Picart, J. C. Voegel, S. Muller and J. F. Stoltz, *Biomaterials*, 2003, **24**, 3521-3530.
137 W. Feng, X. J. Zhou, C. L. He, K. X. Qiu, W. Nie, L. Chen, H. S. Wang, X. M. Mo and Y. Z. Zhang, *J. Mater. Chem. B*, 2013, **1**, 5886-5898.
138 S. T. Dubas, P. Kittitheeranun, R. Rangkupan, N. Sanchavanakit and P. Potiyaraj, *J. Appl. Polym. Sci.*, 2009, **114**, 1574-1579.
139 H. S. Yu, J. H. Jang, T. I. Kim, H. H. Lee and H. W. Kim, *J. Biomed. Mater. Res., Part A*, 2009, **88A**, 747-754.
140 J. L. Chen, B. Chu and B. S. Hsiao, *J. Biomed. Mater. Res., Part A*, 2006, **79A**, 307-317.
141 S. Patel, K. Kurpinski, R. Quigley, H. F. Gao, B. S. Hsiao, M. M. Poo and S. Li, *Nano Lett.*, 2007, **7**, 2122-2128.
142 T. G. Kim and T. G. Park, *Tissue Eng.*, 2006, **12**, 221-233.
143 W. S. Li, Y. Guo, H. Wang, D. J. Shi, C. F. Liang, Z. P. Ye, F. Qing and J. Gong, *J. Mater. Sci.: Mater. Med.*, 2008, **19**, 847-854.
144 D. Grafahrend, K. H. Heffels, M. V. Beer, P. Gasteier, M. Moller, G. Boehm, P. D. Dalton and J. Groll, *Nat. Mater.*, 2011, **10**, 67-73.
145 K. Klinkhammer, J. Bockelmann, C. Simitzis, G. A. Brook, D. Grafahrend, J. Groll, M. Moller, J. Mey and D. Klee, *J. Mater. Sci.: Mater. Med.*, 2010, **21**, 2637-2651.
146 M. Zhang, Z. X. Wang, Z. F. Wang, S. R. Feng, H. J. Xu, Q. Zhao, S. F. Wang, J. X. Fang, M. Q. Qiao and D. L. Kong, *Colloids Surf., B*, 2011, **85**, 32-39.
147 C. L. Casper, N. Yamaguchi, K. L. Kiick and J. F. Rabolt, *Biomacromolecules*, 2005, **6**, 1998-2007.
148 W. H. Lin and W. B. Tsai, *Biofabrication*, 2013, **5**, 035008.
149 J. Ratanavaraporn, R. Rangkupan, H. Jeeratawatchai, S. Kanokpanont and S. Damrongsakkul, *Int. J. Biol. Macromol.*, 2010, **47**, 431-438.
150 S. P. Zhong, W. E. Teo, X. Zhu, R. W. Beuerman, S. Ramakrishna and L. Y. L. Yung, *J. Biomed. Mater. Res., Part A*, 2006, **79A**, 456-463.
151 K. J. Shields, M. J. Beckman, G. L. Bowlin and J. S. Wayne, *Tissue Eng.*, 2004, **10**, 1510-1517.
152 L. Buttafoco, N. G. Kolkman, P. Engbers-Buijtenhuijs, A. A. Poot, P. J. Dijkstra, I. Vermes and J. Feijen, *Biomaterials*, 2006, **27**, 724-734.
153 Y. Z. Zhang, J. Venugopal, Z. M. Huang, C. T. Lim and S. Ramakrishna, *Polymer*, 2006, **47**, 2911-2917.
154 S. Panzavolta, M. Gioffre, M. L. Focarete, C. Gualandi, L. Foroni and A. Bigi, *Acta Biomater.*, 2011, **7**, 1702-1709.
155 K. Sisson, C. Zhang, M. C. Farach-Carson, D. B. Chase and J. F. Rabolt, *Biomacromolecules*, 2009, **10**, 1675-1680.
156 H. Y. Wang, Y. K. Feng, Z. C. Fang, R. F. Xiao, W. J. Yuan and M. Khan, *Macromol. Res.*, 2013, **21**, 860-869.
157 M. C. McManus, E. D. Boland, D. G. Simpson, C. P. Barnes and G. L. Bowlin, *J. Biomed. Mater. Res., Part A*, 2007, **81A**, 299-309.
158 I. S. Yeo, J. E. Oh, L. Jeong, T. S. Lee, S. J. Lee, W. H. Park and B. M. Min, *Biomacromolecules*, 2008, **9**, 1106-1116.
159 J. L. Vondran, W. Sun and C. L. Schauer, *J. Appl. Polym. Sci.*, 2008, **109**, 968-975.
160 J. D. Schiffman and C. L. Schauer, *Biomacromolecules*, 2007, **8**, 594-601.
161 C. Z. Chen, L. G. Wang and Y. Huang, *Mater. Lett.*, 2009, **63**, 569-571.
162 P. Van Wachem, M. Van Luyn, L. Damink, P. Dijkstra, J. Feijen and P. Nieuwenhuis, *J. Biomed. Mater. Res.*, 1994, **28**, 353-363.
163 A. Jayakrishnan and S. R. Jameela, *Biomaterials*, 1996, **17**, 471-484.
164 P. L. Field, *Cardiovasc. Surg.*, 2003, **11**, 30-34.
165 M. K. Widmer, F. Aregger, E. Stauffer, H. Savolainen, G. Heller, H. Hakki, T. Carrel, J. Schmidli and M. G. Mohaupt, *Eur. J. Vasc. Endovasc.*, 2004, **27**, 660-665.
166 C. P. Barnes, C. W. Pemble, D. D. Brand, D. G. Simpson and G. L. Bowlin, *Tissue Eng.*, 2007, **13**, 1593-1605.
167 J. H. Ko, H. Yin, J. An, D. J. Chung, J. H. Kim, S. B. Lee and D. G. Pyun, *Macromol. Res.*, 2010, **18**, 137-143.
168 R. Ravichandran, V. Seitz, J. R. Venugopal, R. Sridhar, S. Sundarrajan, S. Mukherjee, E. Wintermantel and S. Ramakrishna, *Macromol. Biosci.*, 2013, **13**, 366-375.
169 C. Gao, Y. Z. Wan, X. W. Lei, J. Qu, T. Yan and K. R. Dai, *Cellulose*, 2011, **18**, 1555-1561.
170 C. H. Yao, B. S. Liu, C. J. Chang, S. H. Hsu and Y. S. Chen, *Mater. Chem. Phys.*, 2004, **83**, 204-208.
171 M. T. Nickerson, R. Farnworth, E. Wagar, S. M. Hodge, D. Rousseau and A. T. Paulson, *Int. J. Biol. Macromol.*, 2006, **38**, 40-44.
172 R. Meena, K. Prasad and A. K. Siddhanta, *Food Hydrocolloids*, 2009, **23**, 497-509.
173 K. Rinki and P. K. Dutta, *Int. J. Biol. Macromol.*, 2010, **46**, 261-266.
174 C. C. Tsai, R. N. Huang, H. W. Sung and H. C. Liang, *J. Biomed. Mater. Res.*, 2000, **52**, 58-65.
175 A. O. Gee, B. M. Baker, A. M. Silverstein, G. Montero, J. L. Esterhai and R. L. Mauck, *Cell Tissue Res.*, 2012, **347**, 803-813.
176 A. J. Bavariya, A. Norowski, K. M. Anderson, P. C. Adatrow, F. Garcia-Godoy, S. H. Stein and J. D. Bumgardner, *J. Biomed. Mater. Res., Part B*, 2014, **102**, 1084-1092.
177 K. H. Zhang, Y. F. Qian, H. S. Wang, L. P. Fan, C. Huang, A. L. Yin and X. M. Mo, *J. Biomed. Mater. Res., Part A*, 2010, **95A**, 870-881.
178 S. S. Silva, D. Maniglio, A. Motta, J. F. Mano, R. L. Reis and C. Migliaresi, *Macromol. Biosci.*, 2008, **8**, 766-774.
179 J. Wang, Y. Z. Wan, H. L. Luo, C. Gao and Y. Huang, *Mater. Sci. Eng., C*, 2012, **32**, 536-541.
180 H. Y. Wang, Y. K. Feng, B. An, W. C. Zhang, M. L. Sun, Z. C. Fang, W. J. Yuan and M. Khan, *J. Mater. Sci.: Mater. Med.*, 2012, **23**, 1499-1510.
181 C. L. He, W. Feng, L. J. Cao and L. P. Fan, *J. Biomed. Mater. Res., Part A*, 2011, **99A**, 655-665.
182 C. M. Li, C. Vepari, H. J. Jin, H. J. Kim and D. L. Kaplan, *Biomaterials*, 2006, **27**, 3115-3124.
183 Y. K. Luu, K. Kim, B. S. Hsiao, B. Chu and M. Hadjiargyrou, *J. Controlled Release*, 2003, **89**, 341-353.
184 S. N. Jayasinghe, *Analyst*, 2013, **138**, 2215-2223.

185 S. L. Sampson, L. Saraiva, K. Gustafsson, S. N. Jayasinghe and B. D. Robertson, *Small*, 2014, **10**, 78-82.
186 E. R. Kenawy, G. L. Bowlin, K. Mansfield, J. Layman, D. G. Simpson, E. H. Sanders and G. E. Wnek, *J. Controlled Release*, 2002, **81**, 57-64.
187 X. H. Zong, S. Li, E. Chen, B. Garlick, K. S. Kim, D. F. Fang, J. Chiu, T. Zimmerman, C. Brathwaite, B. S. Hsiao and B. Chu, *Ann. Surg.*, 2004, **240**, 910-915.
188 H. L. Jiang, D. F. Fang, B. J. Hsiao, B. J. Chu and W. L. Chen, *J. Biomater. Sci., Polym. Ed*, 2004, **15**, 279-296.
189 D. S. Katti, K. W. Robinson, F. K. Ko and C. T. Laurencin, *J. Biomed. Mater. Res., Part B*, 2004, **70B**, 286-296.
190 Z. Jing, X. Y. Xu, X. S. Chen, Q. Z. Liang, X. C. Bian, L. X. Yang and X. B. Jing, *J. Controlled Release*, 2003, **92**, 227-231.
191 G. Verreck, I. Chun, J. Peeters, J. Rosenblatt and M. E. Brewster, *Pharm. Res.*, 2003, **20**, 810-817.
192 J. J. Han, S. Farah, A. J. Domb and P. I. Lelkes, *Pharm. Res.*, 2013, **30**, 1735-1748.
193 X. L. Xu, X. S. Chen, X. Y. Xu, T. C. Lu, X. Wang, L. X. Yang and X. B. Jing, *J. Controlled Release*, 2006, **114**, 307-316.
194 F. Y. Zheng, S. G. Wang, M. W. Shen, M. F. Zhu and X. Y. Shi, *Polym. Chem.*, 2013, **4**, 933-941.
195 M. G. Ignatova, N. E. Manolova, R. A. Toshkova, I. B. Rashkov, E. G. Gardeva, L. S. Yossifova and M. T. Alexandrov, *Biomacromolecules*, 2010, **11**, 1633-1645.
196 X. L. Xu, X. S. Chen, P. A. Ma, X. R. Wang and X. B. Jing, *Eur. J. Pharm. Biopharm.*, 2008, **70**, 165-170.
197 X. L. Xu, L. X. Yang, X. Y. Xu, X. Wang, X. S. Chen, Q. Z. Liang, J. Zeng and X. B. Jing, *J. Controlled Release*, 2005, **108**, 33-42.
198 J. W. Xie, R. S. Tan and C. H. Wang, *J. Biomed. Mater. Res., Part A*, 2008, **85A**, 897-908.
199 X. Q. Cai, Y. X. Luan, Q. Dong, W. Shao, Z. H. Li and Z. X. Zhao, *Int. J. Pharm.*, 2011, **419**, 240-246.
200 S. J. Shao, L. Li, G. Yang, J. R. Li, C. Luo, T. Gong and S. B. Zhou, *Int. J. Pharm.*, 2011, **421**, 310-320.
201 S. T. Yohe, V. L. M. Herrera, Y. L. Colson and M. W. Grinstaff, *J. Controlled Release*, 2012, **162**, 92-101.
202 A. Sharma, A. Gupta, G. Rath, A. Goyal, R. B. Mathur and S. R. Dhakate, *J. Mater. Chem. B*, 2013, **1**, 3410-3418.
203 J. Zeng, A. Aigner, F. Czubayko, T. Kissel, J. H. Wendorff and A. Greiner, *Biomacromolecules*, 2005, **6**, 1484-1488.
204 S. Y. Chew, J. Wen, E. K. F. Yim and K. W. Leong, *Biomacromolecules*, 2005, **6**, 2017-2024.
205 E. H. Sanders, R. Kloefkorn, G. L. Bowlin, D. G. Simpson and G. E. Wnek, *Macromolecules*, 2003, **36**, 3803-3805.
206 K. Kim, Y. K. Luu, C. Chang, D. F. Fang, B. S. Hsiao, B. Chu and M. Hadjiargyrou, *J. Controlled Release*, 2004, **98**, 47-56.
207 K. X. Qiu, C. L. He, W. Feng, W. Z. Wang, X. J. Zhou, Z. Q. Yin, L. Chen, H. S. Wang and X. M. Mo, *J. Mater. Chem. B*, 2013, **1**, 4601-4611.
208 R. L. Qi, R. Guo, M. W. Shen, X. Y. Cao, L. Q. Zhang, J. J. Xu, J. Y. Yu and X. Y. Shi, *J. Mater. Chem.*, 2010, **20**, 10622-10629.
209 H. Jiang, L. Wang and K. Zhu, *J. Controlled Release*, 2014, DOI: 10.1016/j.jconrel.2014.04.025.
210 H. L. Jiang, Y. Q. Hu, Y. Li, P. C. Zhao, K. J. Zhu and W. L. Chen, *J. Controlled Release*, 2005, **108**, 237-243.
211 X. Q. Li, Y. Su, R. Chen, C. L. He, H. S. Wang and X. M. Mo, *J. Appl. Polym. Sci.*, 2009, **111**, 1564-1570.
212 H. Zhang, X. L. Jia, F. X. Han, J. Zhao, Y. H. Zhao, Y. B. Fan and X. Y. Yuan, *Biomaterials*, 2013, **34**, 2202-2212.
213 X. L. Jia, C. G. Zhao, P. Li, H. Zhang, Y. Huang, H. Li, J. Fan, W. Feng, X. Y. Yuan and Y. B. Fan, *J. Biomater. Sci., Polym. Ed*, 2011, **22**, 1811-1827.
214 I. C. Liao, S. Y. Chew and K. W. Leong, *Nanomedicine*, 2006, **1**, 465-471.
215 H. Li, C. G. Zhao, Z. X. Wang, H. Zhang, X. Y. Yuan and D. L. Kong, *J. Biomater. Sci., Polym. Ed*, 2010, **21**, 803-819.
216 S. Sahoo, L. T. Ang, J. C. H. Goh and S. L. Toh, *J. Biomed. Mater. Res., Part A*, 2010, **93A**, 1539-1550.
217 H. X. Qi, P. Hu, J. Xu and A. J. Wang, *Biomacromolecules*, 2006, **7**, 2327-2330.
218 Y. Yang, X. H. Li, M. B. Qi, S. B. Zhou and J. Weng, *Eur. J. Pharm. Biopharm.*, 2008, **69**, 106-116.
219 B. S. Kim, J. M. Oh, K. S. Kim, K. S. Seo, J. S. Cho, G. Khang, H. B. Lee, K. Park and M. S. Kim, *Biomaterials*, 2009, **30**, 902-909.
220 G. B. Wei, Q. M. Jin, W. V. Giannobile and P. X. Ma, *J. Controlled Release*, 2006, **112**, 103-110.
221 J. Hu and P. X. Ma, *Pharm. Res.*, 2011, **28**, 1273-1281.
222 W. G. Cui, X. H. Li, X. L. Zhu, G. Yu, S. B. Zhou and J. Weng, *Biomacromolecules*, 2006, **7**, 1623-1629.
223 G. Buschle-Diller, J. Cooper, Z. W. Xie, Y. Wu, J. Waldrup and X. H. Ren, *Cellulose*, 2007, **14**, 553-562.
224 T. Okuda, K. Tominaga and S. Kidoaki, *J. Controlled Release*, 2010, **143**, 258-264.
225 P. Taepaiboon, U. Rungsardthong and P. Supaphol, *Nanotechnology*, 2006, **17**, 2317-2329.
226 J. W. Xie and C. H. Wang, *Pharm. Res.*, 2006, **23**, 1817-1826.
227 Z. W. Xie and G. Buschle-Diller, *J. Appl. Polym. Sci.*, 2010, **115**, 1-8.
228 J. Zeng, L. X. Yang, Q. Z. Liang, X. F. Zhang, H. L. Guan, X. L. Xu, X. S. Chen and X. B. Jing, *J. Controlled Release*, 2005, **105**, 43-51.
229 M. Zamani, M. Morshed, J. Varshosaz and M. Jannesari, *Eur. J. Pharm. Biopharm.*, 2010, **75**, 179-185.
230 R. A. Thakur, C. A. Florek, J. Kohn and B. B. Michniak, *Int. J. Pharm.*, 2008, **364**, 87-93.
231 R. Langer and N. A. Peppas, *AIChE J.*, 2003, **49**, 2990-3006.
232 A. K. Bajpai, S. K. Shukla, S. Bhanu and S. Kankane, *Prog. Polym. Sci.*, 2008, **33**, 1088-1118.
233 T. Nitanan, P. Akkaramongkolporn, T. Ngawhirunpat, T. Rojanarata, S. Panomsuk and P. Opanasopit, *Int. J. Pharm.*, 2013, **450**, 345-353.
234 P. Zahedi, I. Rezaeian, S. H. Jafari and Z. Karami, *Macromol. Res.*, 2013, **21**, 649-659.
235 G. Verreck, I. Chun, J. Rosenblatt, J. Peeters, A. Van Dijck, J. Mensch, M. Noppe and M. E. Brewster, *J. Controlled Release*, 2003, **92**, 349-360.
236 W. Ji, F. Yang, J. van den Beucken, Z. A. Bian, M. W. Fan, Z. Chen and J. A. Jansen, *Acta Biomater.*, 2010, **6**, 4199-4207.
237 J. H. Jang, O. Castano and H. W. Kim, *Adv. Drug Delivery Rev.*, 2009, **61**, 1065-1083.
238 J. Ma, J. L. Wang, X. Ai and S. M. Zhang, *Biotechnol. Adv.*, 2014, **32**, 744-760.
239 R. L. Dahlin, F. K. Kasper and A. G. Mikos, *Tissue Eng. Part B*, 2011, **17**, 349-364.
240 H. Yoshimoto, Y. M. Shin, H. Terai and J. P. Vacanti, *Biomaterials*,

2003, **24**, 2077-2082.
241 M. Shin, H. Yoshimoto and J. P. Vacanti, *Tissue Eng.*, 2004, **10**, 33-41.
242 Y. Z. Zhang, H. W. Ouyang, C. T. Lim, S. Ramakrishna and Z. M. Huang, *J. Biomed. Mater. Res., Part B*, 2005, **72B**, 156-165.
243 H. W. Kim, H. S. Yu and H. H. Lee, *J. Biomed. Mater. Res., Part A*, 2008, **87A**, 25-32.
244 K. Ma, C. K. Chan, S. Liao, W. Y. K. Hwang, Q. Feng and S. Ramakrishna, *Biomaterials*, 2008, **29**, 2096-2103.
245 H. W. Kim, H. H. Lee and J. C. Knowles, *J. Biomed. Mater. Res., Part A*, 2006, **79A**, 643-649.
246 Y. Z. Zhang, J. R. Venugopal, A. El-Turki, S. Ramakrishna, B. Su and C. T. Lim, *Biomaterials*, 2008, **29**, 4314-4322.
247 C. Erisken, D. M. Kalyon and H. J. Wang, *Biomaterials*, 2008, **29**, 4065-4073.
248 H. W. Kim, J. H. Song and H. E. Kim, *Adv. Funct. Mater.*, 2005, **15**, 1988-1994.
249 G. Sui, X. P. Yang, F. Mei, X. Y. Hu, G. Q. Chen, X. L. Deng and S. Ryu, *J. Biomed. Mater. Res., Part A*, 2007, **82A**, 445-454.
250 T. Kokubo and H. Takadama, *Biomaterials*, 2006, **27**, 2907-2915.
251 W. G. Cui, X. H. Li, C. Y. Xie, H. H. Zhuang, S. B. Zhou and J. Weng, *Biomaterials*, 2010, **31**, 4620-4629.
252 F. Yang, J. G. C. Wolke and J. A. Jansen, *Chem. Eng. J.*, 2008, **137**, 154-161.
253 X. R. Li, J. W. Xie, X. Y. Yuan and Y. N. Xia, *Langmuir*, 2008, **24**, 14145-14150.
254 Y. Ito, H. Hasuda, M. Kamitakahara, C. Ohtsuki, M. Tanihara, I. K. Kang and O. H. Kwon, *J. Biosci. Bioeng.*, 2005, **100**, 43-49.
255 F. Yang, S. K. Both, X. C. Yang, X. F. Walboomers and J. A. Jansen, *Acta Biomater.*, 2009, **5**, 3295-3304.
256 W. G. Cui, X. H. Li, J. G. Chen, S. B. Zhou and J. Weng, *Cryst. Growth Des.*, 2008, **8**, 4576-4582.
257 C. L. He, X. B. Jin and P. X. Ma, *Acta Biomater.*, 2014, **10**, 419-427.
258 C. L. He, G. Y. Xiao, X. B. Jin, C. H. Sun and P. X. Ma, *Adv. Funct. Mater.*, 2010, **20**, 3568-3576.
259 C. L. He, F. Zhang, L. J. Cao, W. Feng, K. X. Qiu, Y. Z. Zhang, H. S. Wang, X. M. Mo and J. W. Wang, *J. Mater. Chem.*, 2012, **22**, 2111-2119.
260 H. M. Nie and C. H. Wang, *J. Controlled Release*, 2007, **120**, 111-121.
261 G. B. Wei, Q. M. Jin, W. V. Giannobile and P. X. Ma, *Biomaterials*, 2007, **28**, 2087-2096.
262 M. J. Gupte and P. X. Ma, *J. Dent. Res.*, 2012, **91**, 227-234.
263 Q. M. Jin, G. B. Wei, Z. Lin, J. V. Sugai, S. E. Lynch, P. X. Ma and W. V. Giannobile, *Plos One*, 2008, **3**, e1729.
264 B. C. Isenberg, C. Williams and R. T. Tranquillo, *Circ. Res.*, 2006, **98**, 25-35.
265 H. M. Nugent and E. R. Edelman, *Circ. Res.*, 2003, **92**, 1068-1078.
266 J. Stitzel, L. Liu, S. J. Lee, M. Komura, J. Berry, S. Soker, G. Lim, M. Van Dyke, R. Czerw, J. J. Yoo and A. Atala, *Biomaterials*, 2006, **27**, 1088-1094.
267 A. Hasan, A. Memic, N. Annabi, M. Hossain, A. Paul, M. R. Dokmeci, F. Dehghani and A. Khademhosseini, *Acta Biomater.*, 2014, **10**, 11-25.
268 W. He, T. Yong, W. E. Teo, Z. W. Ma and S. Ramakrishna, *Tissue Eng.*, 2005, **11**, 1574-1588.
269 B. Bondar, S. Fuchs, A. Motta, C. Migliaresi and C. J. Kirkpatrick, *Biomaterials*, 2008, **29**, 561-572.
270 S. J. Lee, J. J. Yoo, G. J. Lim, A. Atala and J. Stitze, *J. Biomed. Mater. Res., Part A*, 2007, **83A**, 999-1008.
271 L. Soletti, Y. Hong, J. J. Guan, J. J. Stankus, M. S. El-Kurdi, W. R. Wagner and D. A. Vorp, *Acta Biomater.*, 2010, **6**, 110-122.
272 Y. M. Ju, J. S. Choi, A. Atala, J. J. Yoo and S. J. Lee, *Biomaterials*, 2010, **31**, 4313-4321.
273 C. M. Vaz, S. van Tuijl, C. V. C. Bouten and F. P. T. Baaijens, *Acta Biomater.*, 2005, **1**, 575-582.
274 S. G. Wise, M. J. Byrom, A. Waterhouse, P. G. Bannon, M. K. C. Ng and A. S. Weiss, *Acta Biomater.*, 2011, **7**, 295-303.
275 M. J. McClure, S. A. Sell, D. G. Simpson, B. H. Walpoth and G. L. Bowlin, *Acta Biomater.*, 2010, **6**, 2422-2433.
276 J. J. Stankus, L. Soletti, K. Fujimoto, Y. Hong, D. A. Vorp and W. R. Wagner, *Biomaterials*, 2007, **28**, 2738-2746.
277 J. J. Stankus, J. J. Guan, K. Fujimoto and W. R. Wagner, *Biomaterials*, 2006, **27**, 735-744.
278 A. Townsend-Nicholson and S. N. Jayasinghe, *Biomacromolecules*, 2006, **7**, 3364-3369.
279 J. Hu, C. Q. Xie, H. Y. Ma, B. Yang, P. X. Ma and Y. E. Chen, *Plos One*, 2012, **7**, e35580.
280 Y. Wang, J. Hu, J. Jiao, Z. Liu, Z. Zhou, C. Zhao, L.-J. Chang, Y. E. Chen, P. X. Ma and B. Yang, *Biomaterials*, 2014, **35**, 8960-8969.
281 J. A. Hu, X. A. Sun, H. Y. Ma, C. Q. Xie, Y. E. Chen and P. X. Ma, *Biomaterials*, 2010, **31**, 7971-7977.
282 C. Q. Xie, J. Hu, H. Y. Ma, J. F. Zhang, L. J. Chang, Y. E. Chen and P. X. Ma, *Biomaterials*, 2011, **32**, 4369-4375.
283 W. Z. Wang, J. W. Hu, C. L. He, W. Nie, W. Feng, K. X. Qiu, X. J. Zhou, Y. Gao and G. Q. Wang, *J. Biomed. Mater. Res., Part A*, 2014, DOI: 10.1002/jbm.a.35315.
284 A. L. Sieminski, C. E. Semino, H. Gong and R. D. Kamm, *J. Biomed. Mater. Res., Part A*, 2008, **87A**, 494-504.
285 H. Cho, S. Balaji, A. Q. Sheikh, J. R. Hurley, Y. F. Tian, J. H. Collier, T. M. Crombleholme and D. A. Narmoneva, *Acta Biomater.*, 2012, **8**, 154-164.
286 D. A. Narmoneva, O. Oni, A. L. Sieminski, S. G. Zhang, J. P. Gertler, R. D. Kamm and R. T. Lee, *Biomaterials*, 2005, **26**, 4837-4846.
287 A. L. Sieminski, A. S. Was, G. Kim, H. Gong and R. D. Kamm, *Cell Biochem. Biophys.*, 2007, **49**, 73-83.
288 A. Andukuri, W. P. Minor, M. Kushwaha, J. M. Anderson and H. W. Jun, *Nanomedicine (N. Y., NY, U. S.)*, 2010, **6**, 289-297.
289 J. P. Jung, J. L. Jones, S. A. Cronier and J. H. Collier, *Biomaterials*, 2008, **29**, 2143-2151.
290 C. E. Schmidt and J. B. Leach, *Annu. Rev. Biomed. Eng.*, 2003, **5**, 293-347.
291 J. W. Xie, M. R. MacEwan, A. G. Schwartz and Y. N. Xia, *Nanoscale*, 2010, **2**, 35-44.
292 A. Subramanian, U. M. Krishnan and S. Sethuraman, *J. Biomed. Sci. (London, U. K.)*, 2009, **16**, 108.
293 M. P. Prabhakaran, J. R. Venugopal, T. Ter Chyan, L. B. Hai, C. K. Chan, A. Y. Lim and S. Ramakrishna, *Tissue Eng. Part A*, 2008, **14**, 1787-1797.
294 E. Schnell, K. Klinkhammer, S. Balzer, G. Brook, D. Klee, P. Dalton and J. Mey, *Biomaterials*, 2007, **28**, 3012-3025.
295 J. M. Corey, D. Y. Lin, K. B. Mycek, Q. Chen, S. Samuel, E. L. Feldman and D. C. Martin, *J. Biomed. Mater. Res., Part A*, 2007, **83A**, 636-645.
296 J. W. Xie, S. M. Willerth, X. R. Li, M. R. Macewan, A. Rader, S. E.

Sakiyama-Elbert and Y. N. Xia, *Biomaterials*, 2009, **30**, 354-362.
297 S. Y. Chew, R. Mi, A. Hoke and K. W. Leong, *Biomaterials*, 2008, **29**, 653-661.
298 F. Yang, R. Murugan, S. Wang and S. Ramakrishna, *Biomaterials*, 2005, **26**, 2603-2610.
299 X. Jiang, H. Q. Cao, L. Y. Shi, S. Y. Ng, L. W. Stanton and S. Y. Chew, *Acta Biomater.*, 2012, **8**, 1290-1302.
300 J. W. Xie, M. R. MacEwan, X. R. Li, S. E. Sakiyama-Elbert and Y. N. Xia, *Acs Nano*, 2009, **3**, 1151-1159.
301 J. W. Xie, W. Y. Liu, M. R. MacEwan, P. C. Bridgman and Y. N. Xia, *Acs Nano*, 2014, **2**, 1778-1785.
302 S. Y. Chew, R. F. Mi, A. Hoke and K. W. Leong, *Adv. Funct. Mater.*, 2007, **17**, 1288-1296.
303 Y. T. Kim, V. K. Haftel, S. Kumar and R. V. Bellamkonda, *Biomaterials*, 2008, **29**, 3117-3127.
304 V. J. Mukhatyar, M. Salmeron-Sanchez, S. Rudra, S. Mukhopadaya, T. H. Barker, A. J. Garcia and R. V. Bellamkonda, *Biomaterials*, 2011, **32**, 3958-3968.
305 J. Y. Lee, C. A. Bashur, C. A. Milroy, L. Forciniti, A. S. Goldstein and C. E. Schmidt, *Ieee T. Nanobiosci.*, 2012, **11**, 15-21.
306 M. K. Horne, D. R. Nisbet, J. S. Forsythe and C. L. Parish, *Stem Cells Dev.*, 2010, **19**, 843-852.
307 Y. Liu, X. Liu, J. Chen, K. J. Gilmore and G. G. Wallace, *Chem. Commun.*, 2008, 3729-3731.
308 J. W. Xie, M. R. MacEwan, S. M. Willerth, X. R. Li, D. W. Moran, S. E. Sakiyama-Elbert and Y. N. Xia, *Adv. Funct. Mater.*, 2009, **19**, 2312-2318.
309 S. H. Bhang, S. I. Jeong, T. J. Lee, I. Jun, Y. B. Lee, B. S. Kim and H. Shin, *Macromol. Biosci.*, 2012, **12**, 402-411.
310 M. Kabiri, M. Soleimani, I. Shabani, K. Futrega, N. Ghaemi, H. H. Ahvaz, E. Elahi and M. R. Doran, *Biotechnol. Lett.*, 2012, **34**, 1357-1365.
311 J. Y. Lee, C. A. Bashur, A. S. Goldstein and C. E. Schmidt, *Biomaterials*, 2009, **30**, 4325-4335.
312 J. D. Tovar, B. M. Rabatic and S. I. Stupp, *Small*, 2007, **3**, 2024-2028.
313 K. Tashiro, G. C. Sephel, B. Weeks, M. Sasaki, G. R. Martin, H. K. Kleinman and Y. Yamada, *J. Biol. Chem.*, 1989, **264**, 16174-16182.
314 W. Q. Liu, J. A. Martinez, J. Durand, W. Wildering and D. W. Zochodne, *Neurobiol. Dis.*, 2009, **34**, 11-22.
315 F. Gelain, D. Bottai, A. Vescovi and S. G. Zhang, *Plos One*, 2006, **1**, e119.
316 R. G. Ellis-Behnke, Y. X. Liang, S. W. You, D. K. C. Tay, S. G. Zhang, K. F. So and G. E. Schneider, *Proc. Natl. Acad. Sci. U. S. A.*, 2006, **103**, 5054-5059.
317 J. Guo, H. Su, Y. Zeng, Y. X. Liang, W. M. Wong, R. G. Ellis-Behnke, K. F. So and W. Wu, *Nanomedicine (N. Y., NY, U. S.)*, 2007, **3**, 311-321.
318 P. D. Dalton, C. Vaquette, B. L. Farrugia, T. R. Dargaville, T. D. Brown and D. W. Hutmacher, *Biomater. Sci.*, 2013, **1**, 171-185.

Figure Captions

Fig. 1. Schematic of the ECM. The major ECM components such as collagen and elastin exist in the form of interwoven nanofibers, which provides a fibrillar matrix network to support cells and direct their behavior. Cells interact with their ECM microenvironments by receptor-mediated interactions, the sequestration of growth factors by the ECM, spatial cues and mechanical force transduction, to trigger various intracellular signaling pathways that regulate various essential cell behaviors and cell fate determination.

Fig. 2. Schematic of different electrospinning apparatus and the fabricated electrospun nanofibers. (a) Typical electrospinning apparatus. (b) Multiple spinneret electrospinning setup. (c) Coaxial electrospinning setup used to fabricate core-sheath nanofibers. (d) SEM image of the electrospun PLLA nanofibers. Reproduced with permission from ref. 258. (e) Fluorescent image of the dual-polymer composite fibrous scaffold, which fabricated by using a dual spinneret electrospinning apparatus. Red and green represents the Cell Tracker Red-stained PCL and the fluorescein-stained PEO electrospun fibers respectively. Reproduced with permission from ref. 21. (f) TEM image of the resultant core-sheath nanofibers with tetracycline hydrochloride in the core and PLLA in the sheath. Reproduced with permission from ref. 13.

Fig. 3. Schematic illustration of different collectors for aligned and patterned nanofibers fabrication. (a) Rotating cylinder collector. (b) Rotating wheel collector. (c) Rotating wire drum collector. (d) The collector contained two pieces of conductive silicon stripes separated by a gap. Reproduced with permission from ref. 37. (e) Dark-field optical micrograph of PVP nanofibers collected on top of a gap formed between two silicon stripes. Reproduced with permission from ref. 37. (f) Cylindrical collector with equally spaced circular protrusions (es, electrospinning process; pc, patterned collector). Reproduced with permission from ref. 41. (g) SEM image of the patterned electrospun nanofibers using cylindrical collector with equally spaced circular protrusions. Reproduced with permission from ref. 41.

Fig. 4. Schematic diagram of the phase separation process that generally includes gelation and solvent exchanging procedures.

Fig. 5. Schematic illustration of the molecular self-assembly process using PA or ionic self-complementary peptides as building blocks. (a) The molecular structure of a typical PA molecule, which consists of a bioactive head, hydrophilic peptide sequence and a hydrophobic aliphatic tail. (b) Formation of micelle at the initial phase of the self-assembly process. (c) A cylindrical micelle formed by self-assembly of PA molecules. (d) SEM image of the PA nanofibers by self-assembly. Reproduced with permission from ref. 71. (e) β-Sheet forming short peptides with

alternating ionic complementary properties: peptide sequences of 4 β-sheet 16-mer peptides, including the commercially available RADA16-I (PuraMatrix™). Structure and assembly of RADA16-1 peptide into fibers and nanofibrous scaffolds (electron microscopy image of RADA16-I is shown). Reproduced with permission from ref. 76.

Fig. 6. Schematic illustration of different methods of preparing drug-loaded nanofibers. (a) Post treatment of nanofibers. (b) Immobilization or incorporation of drug-loaded nanocarriers to nanofibers. (c) Co-electrospinning of drug/polymer blends. (d) Coaxial (or emulsion) electrospinning.

Fig. 7. SEM images of mineralized PLLA nanofibrous matrices by SBF incubation and electrodeposition, respectively. (a) Mineralized in 1.5x SBF for 12 days. Reproduced with permission from ref. 257. (b) Mineralized in 1.5x SBF for 30 days. Reproduced with permission from ref. 257. (c) Electrodeposition at 60 °C and 3V for 30 min. Reproduced with permission from ref. 258. (d) Electrodeposition at 60 °C and 3V for 60 min. Reproduced with permission from ref. 258.

Fig. 8. The living electrospun nanofibers and vessel-like architecture fabricated by cell electrospinning. (a) Nanofibers encapsulated green fluorescent protein (GFP) expressing mouse neuroblastoma N2A cells. Adapted with permission from ref. 185. (b) Fluorescent image of a living vessel-like architecture which generated by using custom made cell electrospinning equipment. (c) Optical micrograph of the cross-section of the vessel-like architecture. (d) Fluorescent image of the inner layer which accommodated endothelial cells. The cells were labelled with dsTomato-expressing lenti-vectors at multiplicity of infection (MOI) 4. (e) Fluorescent image of the outer layer which contained a mixed population of fibroblasts and smooth mussel cells. Cells were labelled with eGFP-containing fusion construct expressing lenti-vectors at MOI 25. (f) The superimposed fluorescent image of the fabricated vessel-like architecture. Adapted from ref. 184 with permission from The Royal Society of Chemistry.

Fig. 9. Fabrication and evaluation of the circumferentially aligned PA tubular gel. (a) The custom made shear chamber contains a glass tube equipped with three O-ring grooves and a stainless steel rod. The glass tube was fixed to a modified 50 mL Falcon tube cap. (b) PA solution loaded in shear chamber. For better visual effect, pyrenebutyric acid was mixed into PA solution, and the photo was taken under UV light. (c) Fabrication procedure showing the inner rod's combined rotation and retraction movement allowing the Ca^{2+} solution to flow into the lumen of the tube. (d) Macroscopic photo of the fabricated PA tube retaining its tubular shape. (e) SEM image of the aligned PA nanofibers on the inner surface of PA tube. (f) SMCs within aligned PA tube visualized by live fluorescence stain after 7 days in culture. (g) Cellular alignment viewed from cross-section of PA tubes after 4 days of culture stained with Alexa Fluor® 568 phalloidin. Adapted with permission from ref. 68.

Fig. 10. The influence of fiber alignment and architecture of the nanofibrous scaffolds on the neurite outgrowth. SEM images of: (a) randomly oriented PCL nanofibers, (c) uniaxially aligned PCL nanofibers, (e) disorder-to-aligned nanofibrous mat, (g) double-layered nanofibrous scaffold with low fiber density. Fluorescence micrographs showing the typical morphology of dorsal root ganglia cultured on: (b) random nanofibers, (d) aligned nanofibers, (f) a border between random and aligned nanofibers, (h) a mat of perpendicular nanofibers. All the nanofibers were coated with laminin. Adapted with permission from ref. 299.

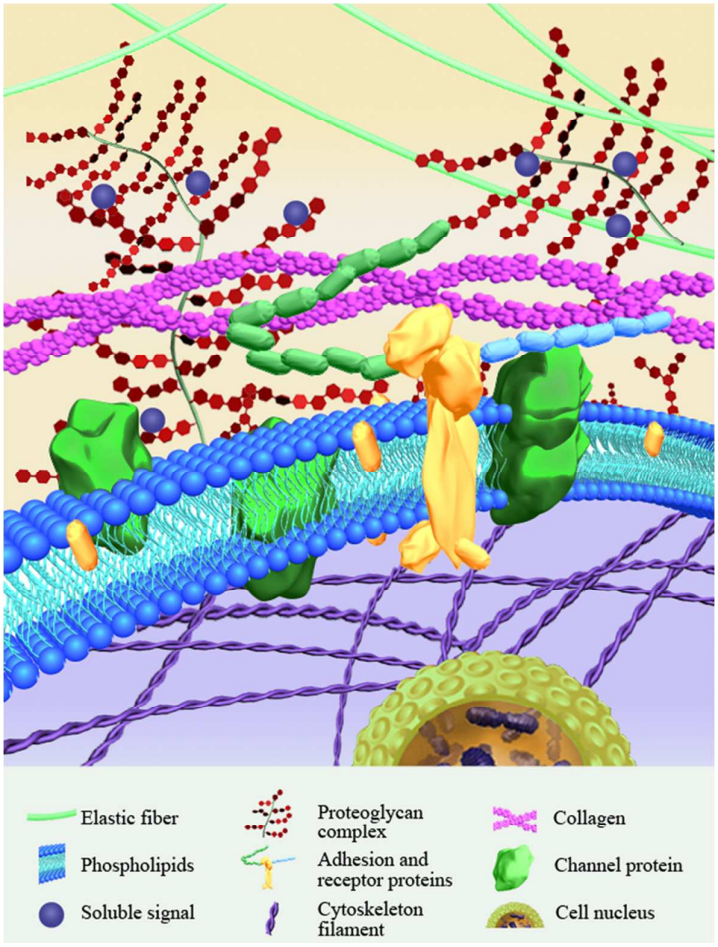

Fig. 1

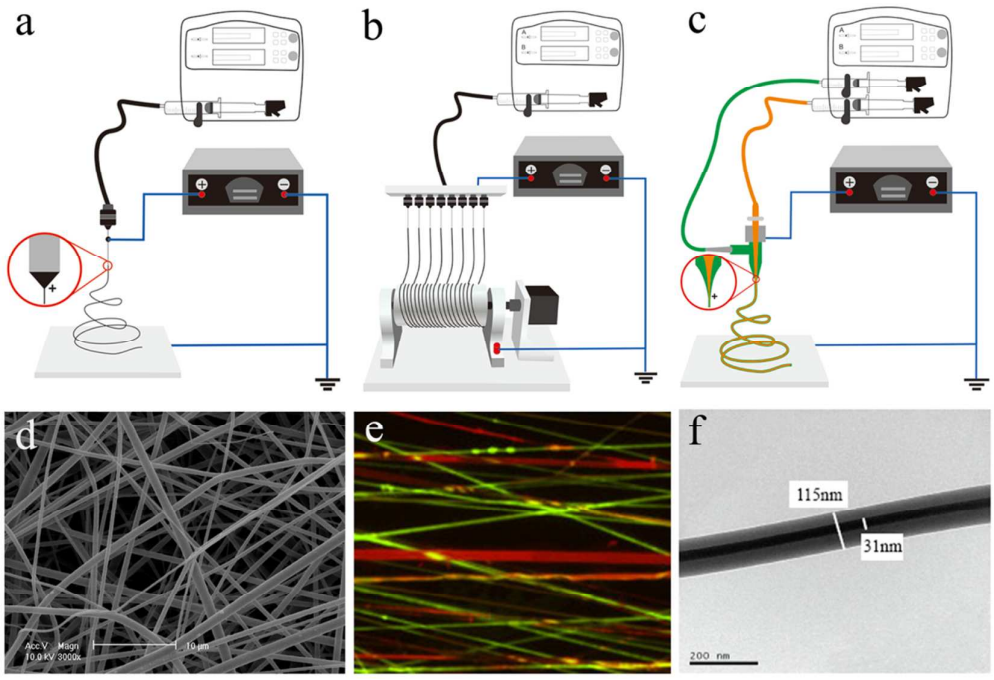

Fig. 2

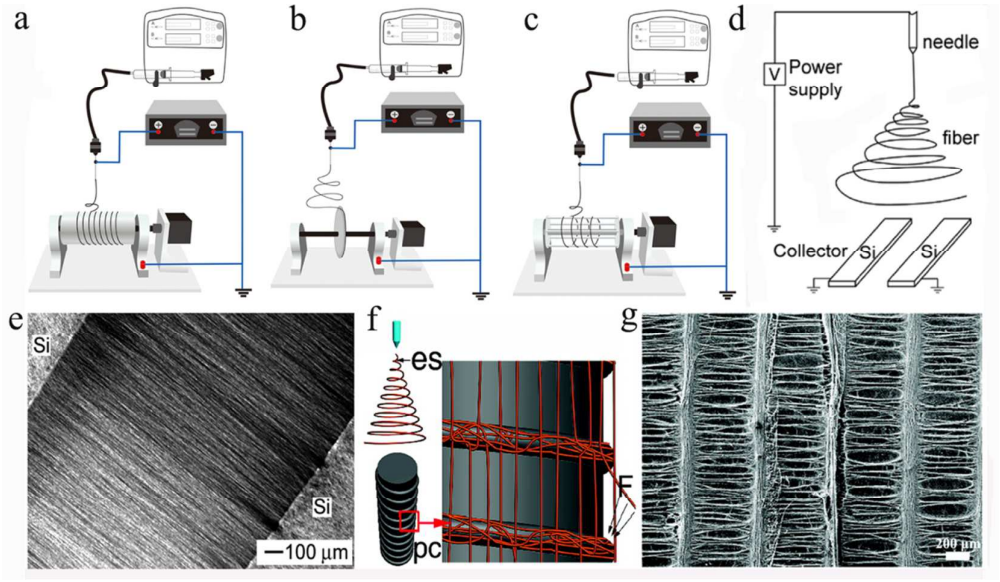

Fig. 3

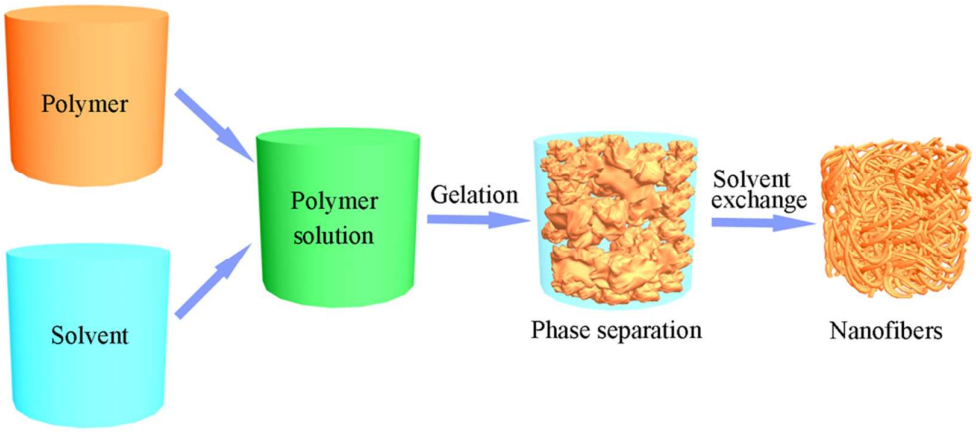

Fig. 4

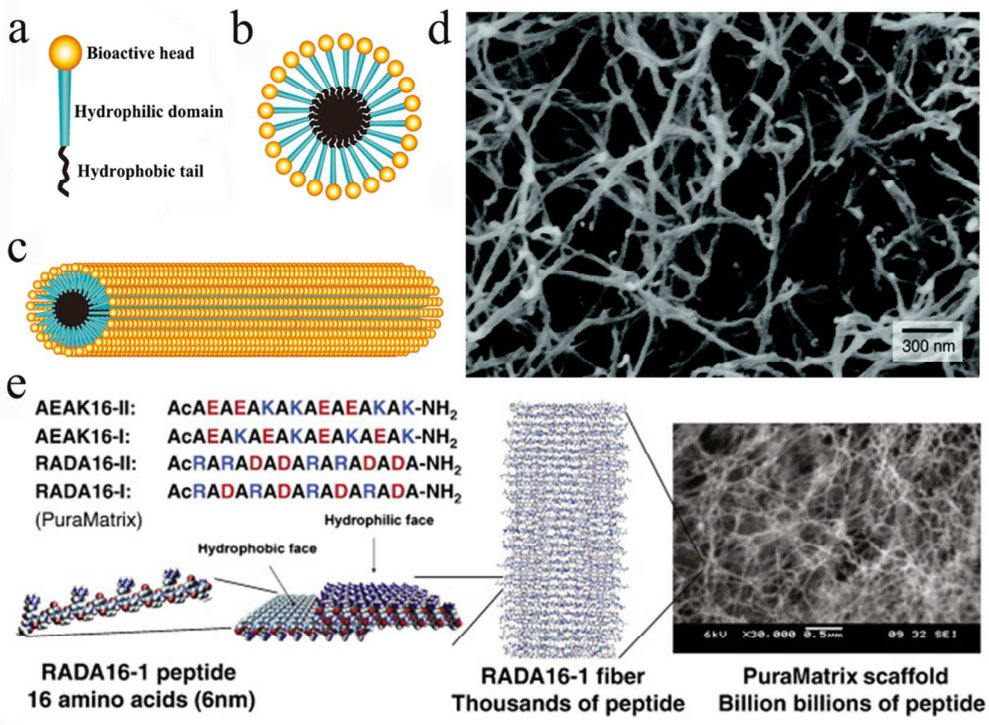

Fig. 5

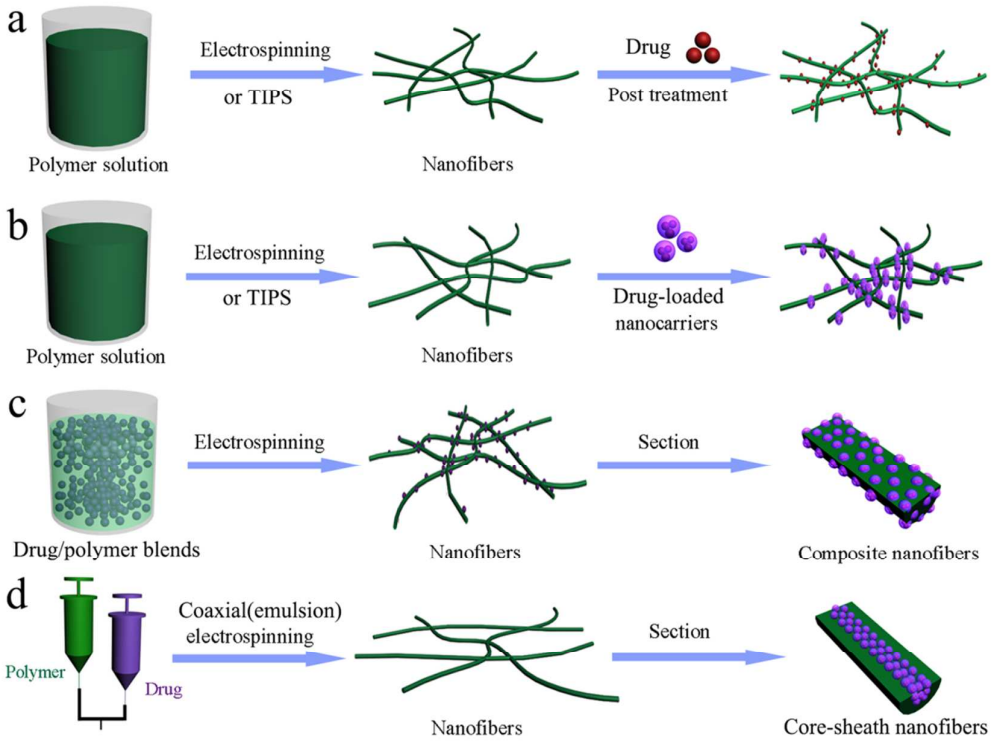

Fig. 6

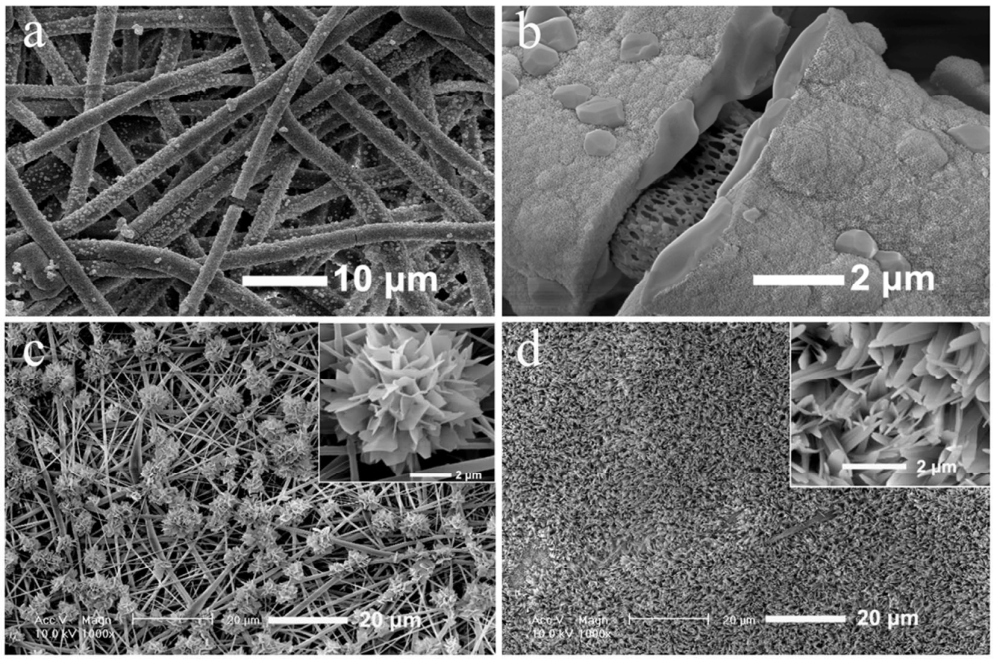

Fig. 7

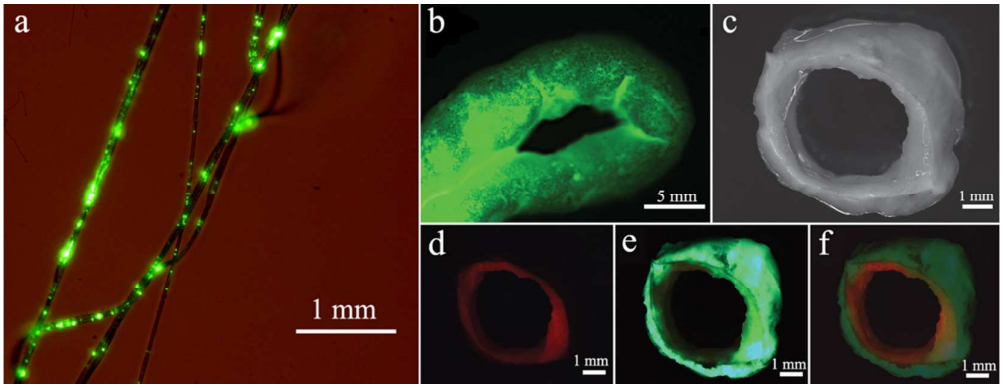

Fig. 8

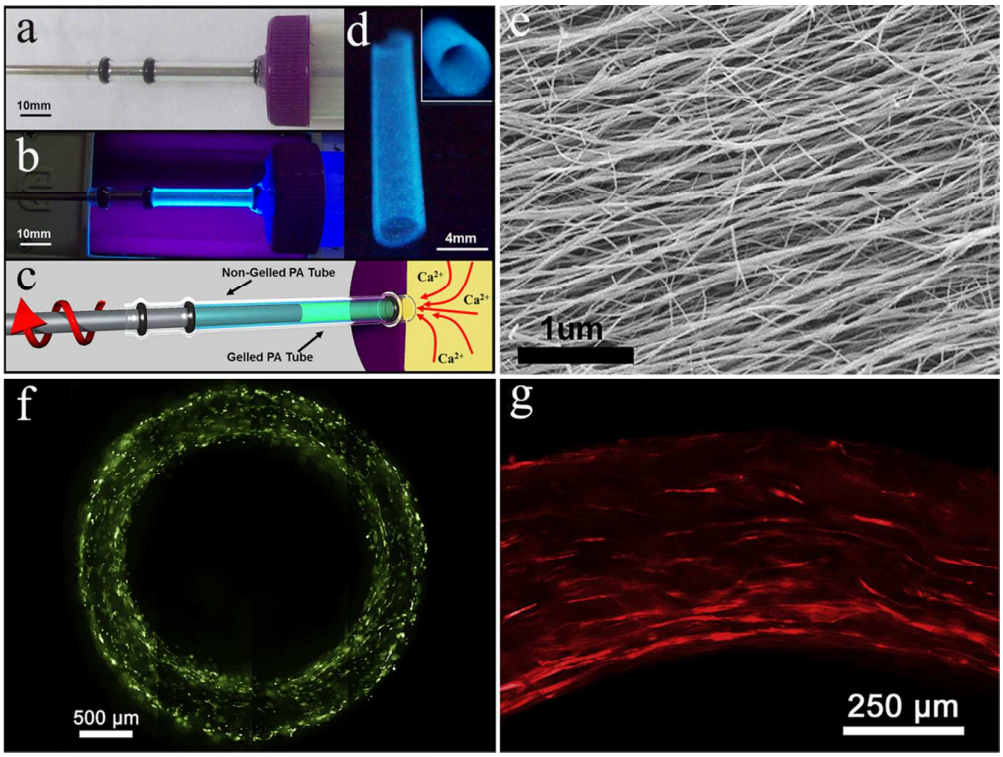

Fig. 9

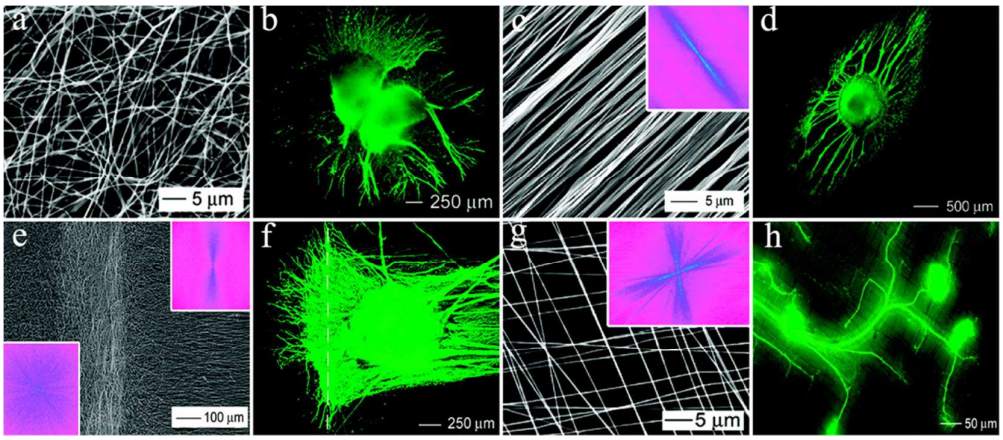

Fig. 10

Graphical abstract

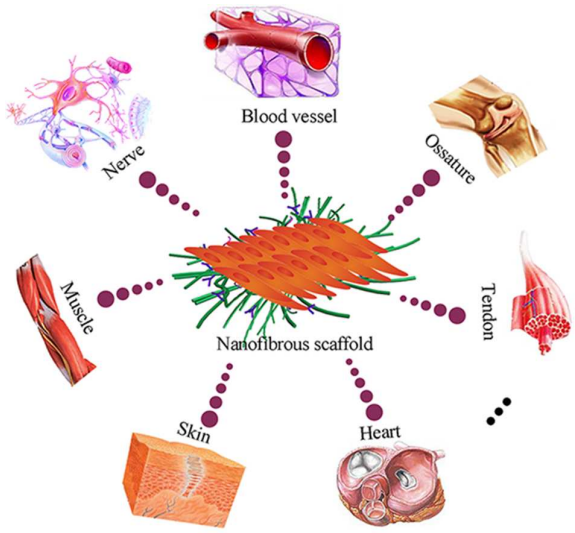

Biomimetic nanofibrous matrices were fabricated by electrospinning, phase separation and molecular self-assembly for drug delivery and tissue engineering applications.